SUPPORTING INFORMATION

PAINS in the assay: chemical mechanisms of assay interference and promiscuous enzymatic inhibition observed during a sulfhydryl-scavenging HTS

Jayme L. Dahlin, J. Willem M. Nissink, Jessica M. Strasser, Subhashree Francis, LeeAnn Higgins, Hui Zhou, Zhiguo Zhang, Michael A. Walters*

Table of contents

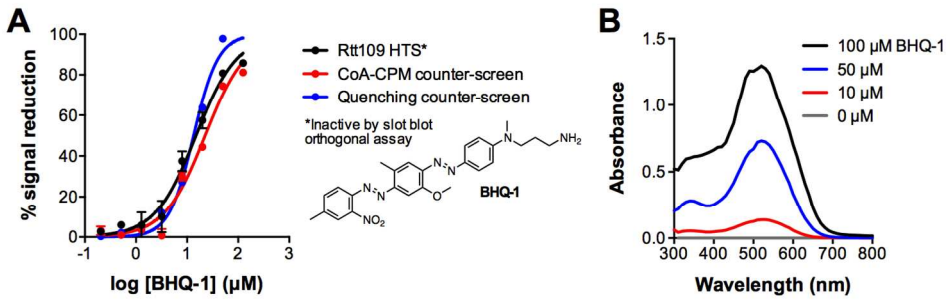

Figure S1 | Characterization of BHQ-1 assay interference. (A) Dose-responses for BHQ-1 using the CPM-based Rtt109 HTS and two counter-screens. The slot blot orthogonal assay demonstrated no inhibition of Rtt109 HAT activity (data not shown). The CoA-CPM counter-screen substitutes the CoA reaction by-product in place of the acetyl-CoA substrate. In the quenching counter-screen, compounds are mixed with pre-formed CoA-CPM adducts. Data are mean ± SD for three replicates. (B) BHQ-1 absorbance spectra in HTS buffer at 30 °C. Note: the CPM-based assay readout wavelength is 530 nm.

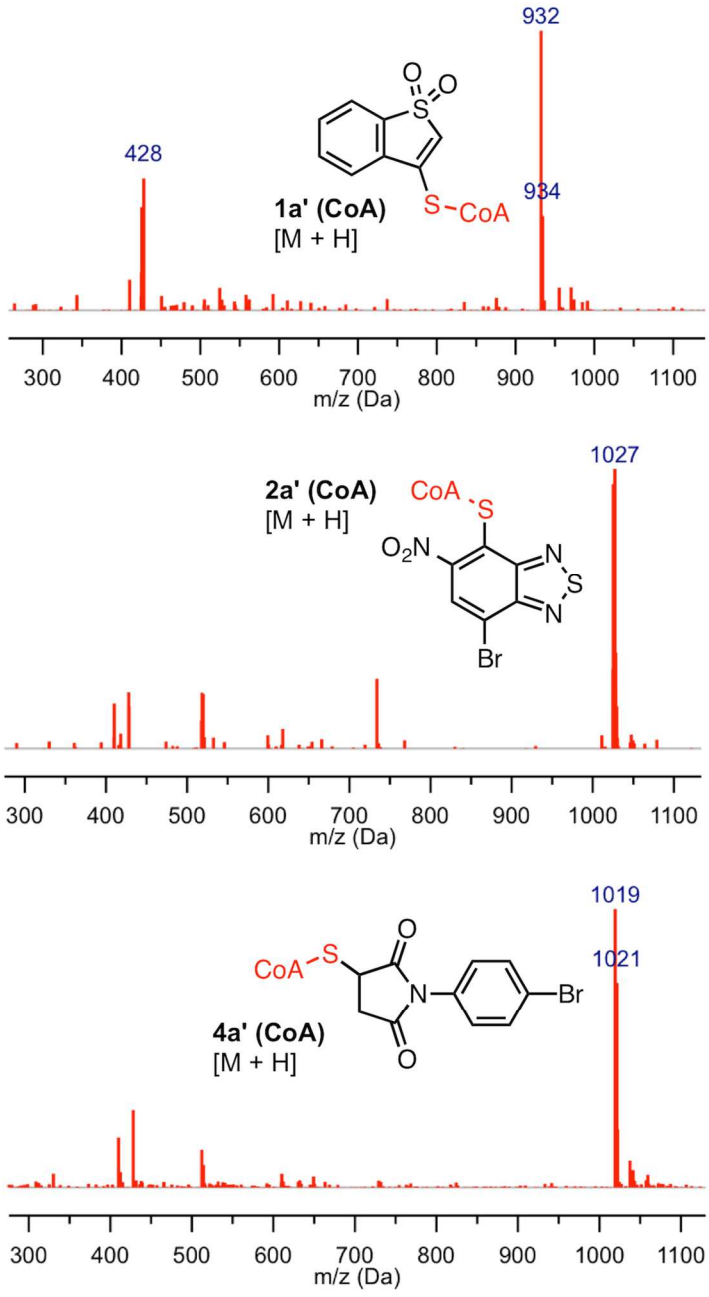

Figure S2 | Examples of compound-CoA adducts detected by UPLC-MS. Selected compounds were incubated with HTS buffer plus CoA and subjected to UPLC-MS analyses. Shown are selected mass spectra of the compound-CoA adducts (positive ion mode), which had similar chromatogram patterns as the corresponding compound-GSH adducts. Data are representative results from one of at least two independent experiments. The structures of the compound-CoA adducts are based on the data for the compound-GSH adducts and the proposed reaction mechanisms (Figure 3 and Supplemental Information).

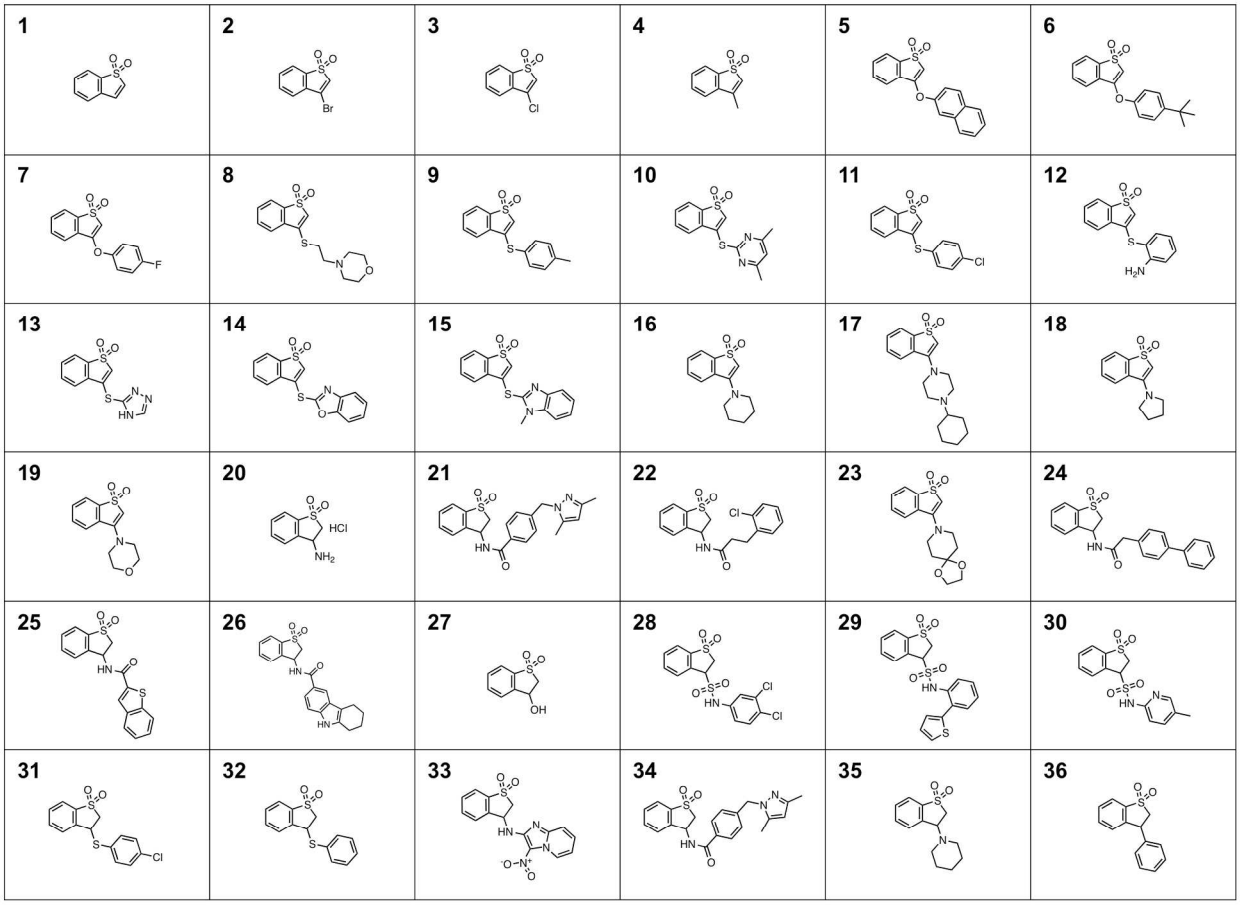

Figure S3 | Inactive and non-interfering compounds related to chemotype 1 (benzothiophene 1,1-dioxides). The compounds shown did not show evidence of Rtt109 inhibition in the CPM-based primary screen (i.e. IC_{50} values > 125 μM) or the orthogonal slot blot assay. The compounds did not demonstrate assay interference in the CoA-CPM interference counter-screen (i.e. IC_{50} values > 125 μM). Table cells are numbered for reference.

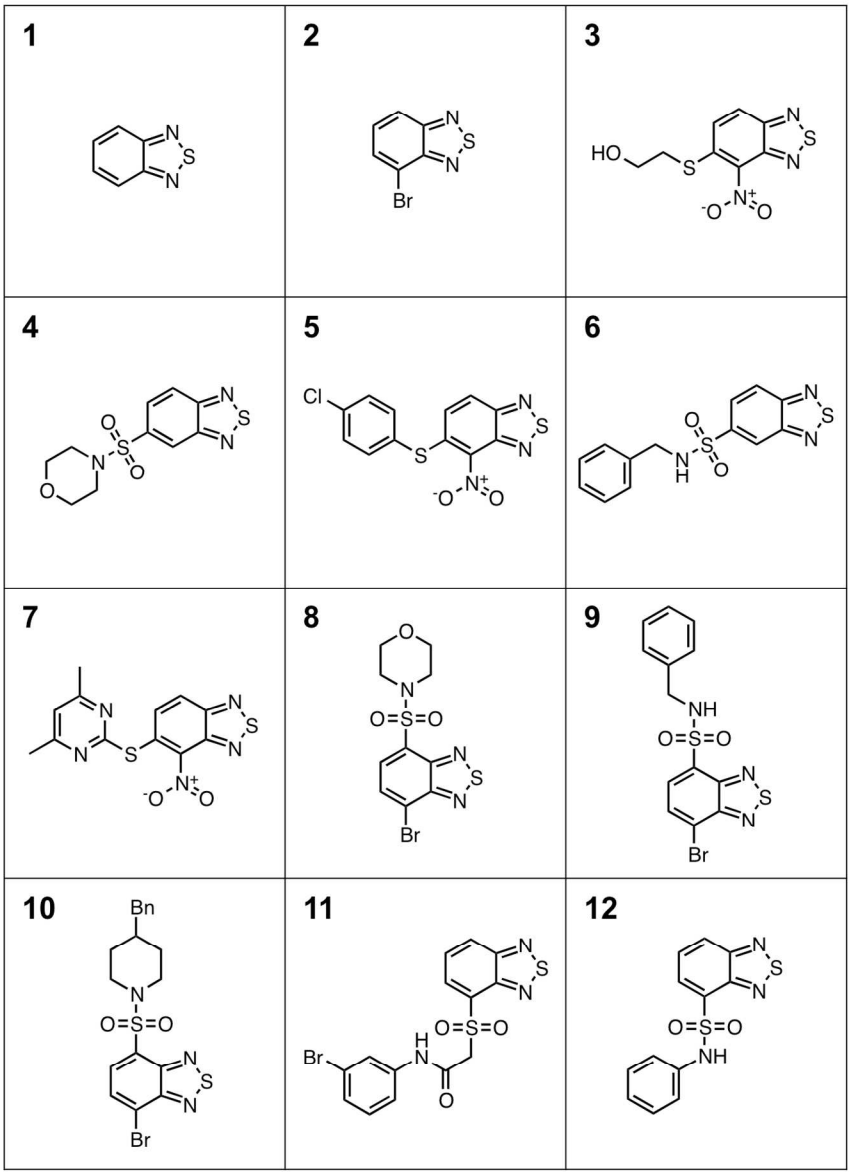

Figure S4 | Inactive and non-interfering compounds related to chemotype 2 (benzothiadiazoles/benzofurazans). The compounds shown did not show evidence of Rtt109 inhibition in the CPM-based primary screen (i.e. IC_{50} values > 125 μM) or the orthogonal slot blot assay. The compounds did not demonstrate assay interference in the CoA-CPM interference counter-screen (i.e. IC_{50} values > 125 μM). Table cells are numbered for reference.

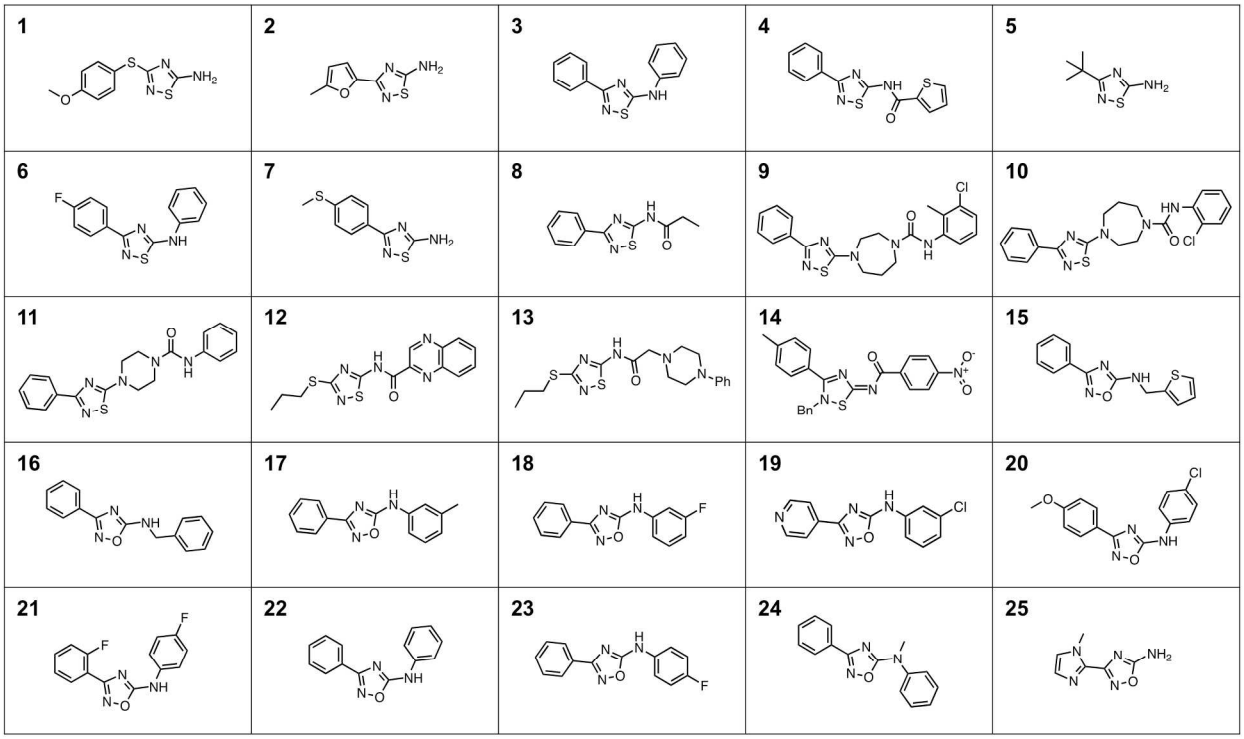

Figure S5 | Inactive and non-interfering compounds related to chemotype 3 (1,2,4-thiadiazoles). The compounds shown did not show evidence of Rtt109 inhibition in the CPM-based primary screen (i.e. IC_{50} values > 125 μM) or the orthogonal slot blot assay. The compounds did not demonstrate assay interference in the CoA-CPM interference counter-screen (i.e. IC_{50} values > 125 μM). Table cells are numbered for reference.

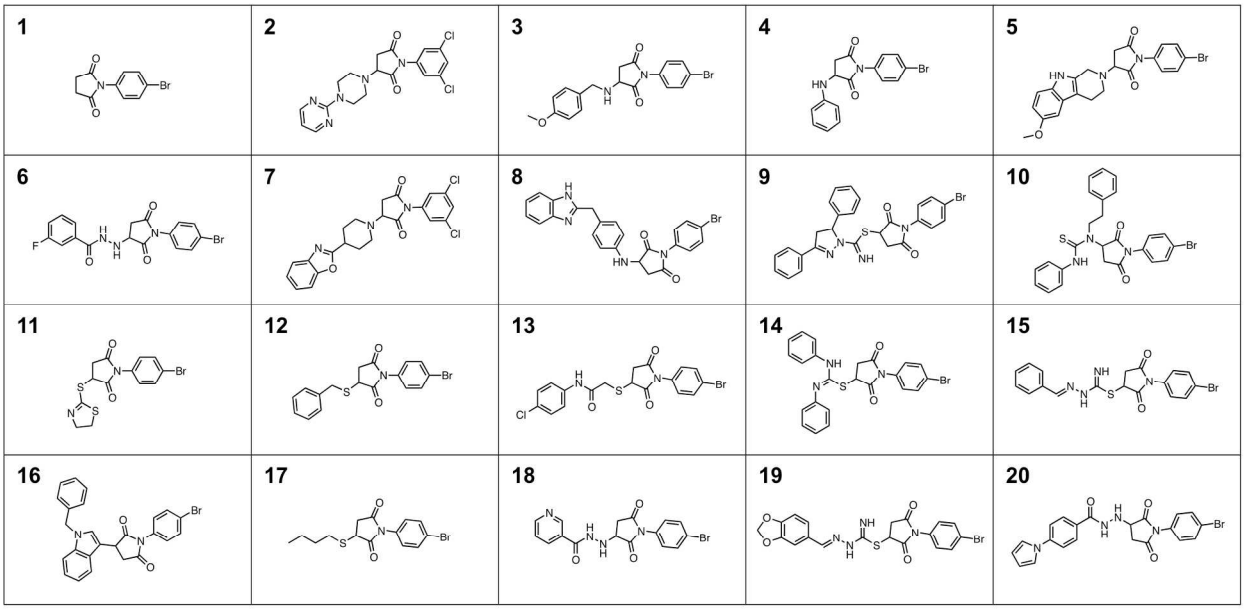

Figure S6 | Inactive and non-interfering compounds related to chemotype 4 (succinimides). The compounds shown did not show evidence of Rtt109 inhibition in the CPM-based primary screen (i.e. IC_{50} values > 125 μM) or the orthogonal slot blot assay. The compounds did not demonstrate assay interference in the CoA-CPM interference counter-screen (i.e. IC_{50} values > 125 μM). Table cells are numbered for reference.

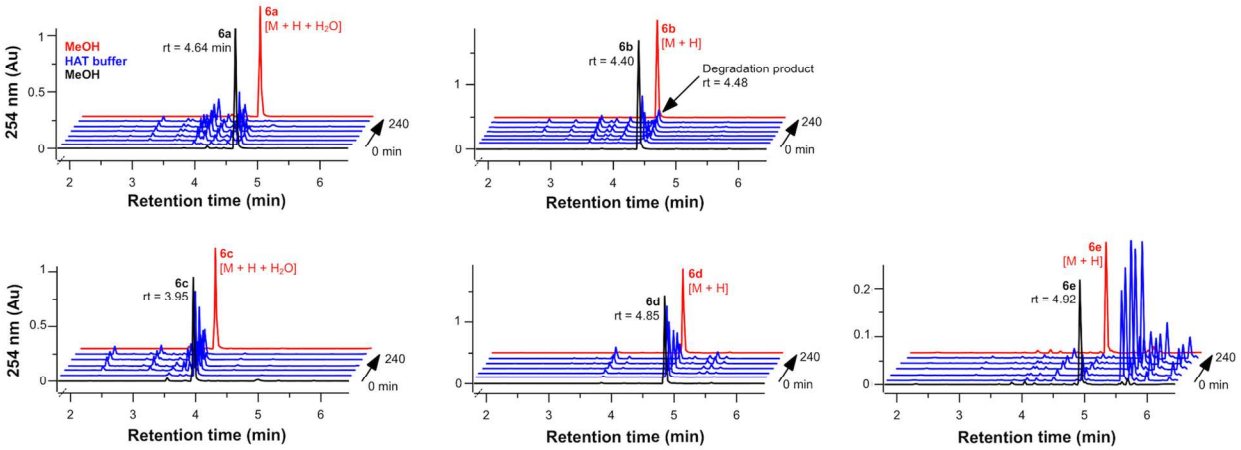

Figure S7 | Qualitative assessments of buffer stability for select *p*-hydroxyarylsulfonamides (6) by UPLC-MS. Sample aliquots were examined over time for evidence of compound instability via absorbance at 254 nm (blue traces). The parent compound peaks were used as retention time (rt) standards (typical variation < 0.01 s between runs). Most of the degradation products did not ionize well under the experimental conditions, hindering further initial characterization. The parent compounds dissolved in MeOH were stable for the entire experiment (0 and 240 min, black and red traces, respectively).

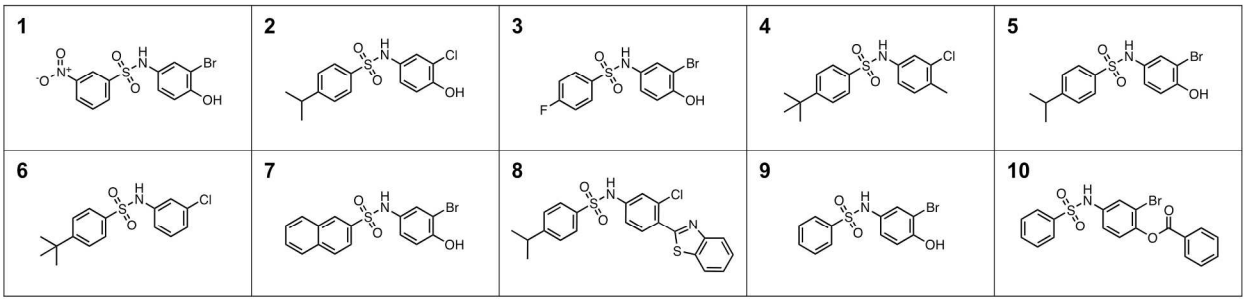

Figure S8 | Inactive and non-interfering compounds (chemotype 7) related to chemotype 6 (*p*-hydroxyarylsulfonamides). The compounds shown did not show evidence of Rtt109 inhibition in the CPM-based primary screen (i.e. IC_{50} values > 125 μM) or the orthogonal slot blot assay. The compounds did not demonstrate assay interference in the CoA-CPM interference counter-screen (i.e. IC_{50} values > 125 μM). Table cells are numbered for reference.

1 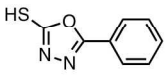 **66 ± 4; 58 ± 2**	2 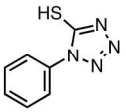 **NR; 86 ± 5**	3 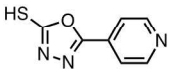 **NR; 250 ± 90**	4 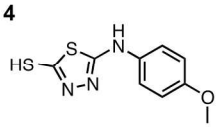 **64 ± 9; 54 ± 2**	5 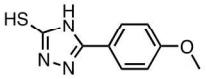 **55 ± 2; 84 ± 5**
6 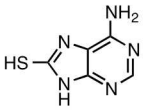 **NR; 220 ± 90**	7 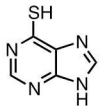 **NR; NR**	8 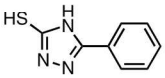 **NR; 280 ± 90**	9 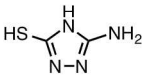 **NR; NR**	10 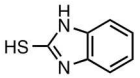 **NR; NR**
11 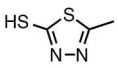 **NR; NR**	12 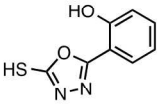 **NR; 160 ± 10**	13 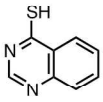 **NR; NR**		**HTS IC_{50}; CoA-CPM counter-screen IC_{50}**

Figure S9 | HTS activity and assay interference of proposed leaving groups in Rtt109 HTS and CoA-CPM counter-screen. All compounds shown did not inhibit Rtt109-Vps75 activity in the orthogonal slot blot assay (data not shown). Additionally, all compounds shown did not produce fluorescent adducts with CPM at compound concentrations tested up to 125 μM or show signs of fluorescent quenching at final compound concentrations of 10 μM. NR; no response. Calculated IC_{50} values shown are means ± SD for three replicates. Table cells are numbered for reference.

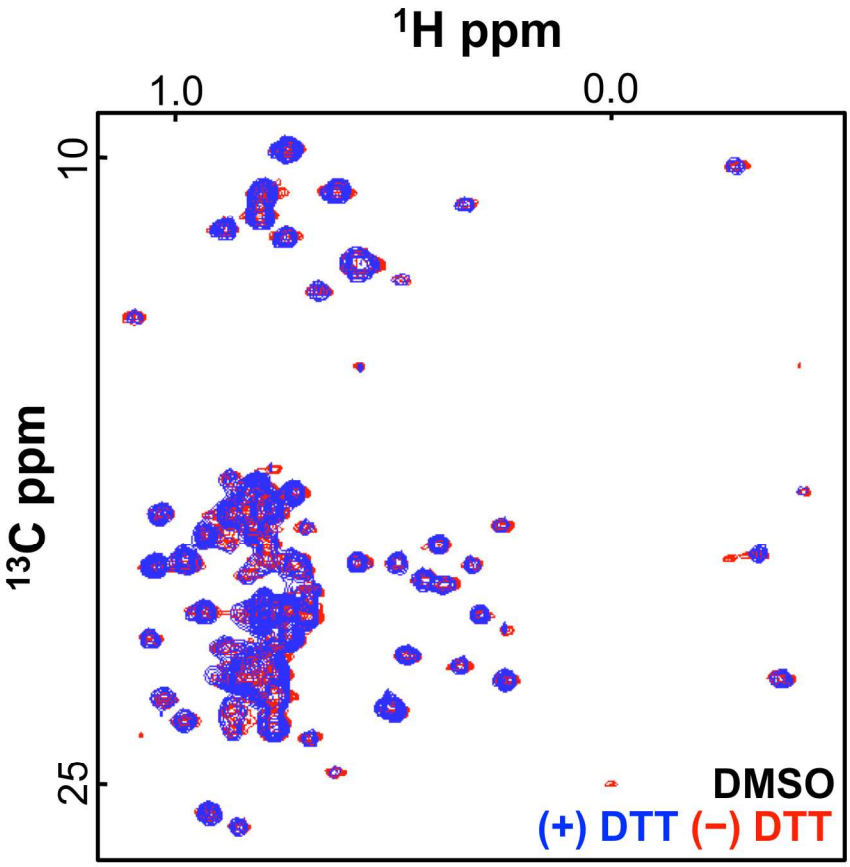

Figure S10 | 2D ^{1}H-^{13}C HMQC spectra for methyl groups of the ALARM NMR protein (La protein, 100-324). Shown is an overlay of the ^{13}C-enriched La protein in the presence (blue) and absence (red) of 20 mM DTT.

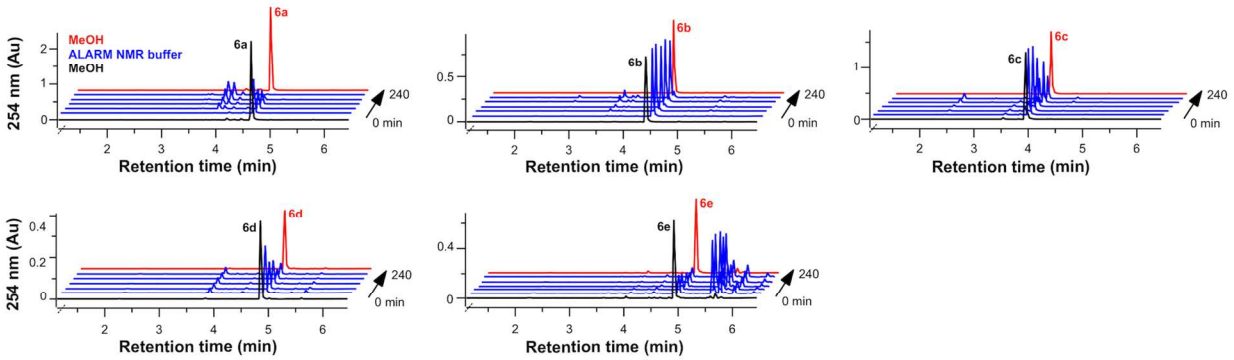

Figure S11 | *p*-Hydroxyarylsulfonamide stabilities in ALARM NMR buffer. Note: compare to Figure S7 for stability in the HTS buffer. Experimental procedures were identical to those used in Figure S7.

Compound	Redox-activity (+) DTT	Redox-activity (−) DTT	Compound	Redox-activity (+) DTT	Redox-activity (−) DTT
1a	−	−	**6o**	−	−
2a	−	−	**6p**	−	−
3a	−	−	**6q**	−	−
4a	−	−	**6r**	−	−
6a	+	+	**6s**	−	+
6b	+	+	**6t**	−	+
6c	+	+	**6u**	−	−
6d	−	−	**6w**	−	−
6e	−	+	**6y**	+	+
6f	+	−	**7a**	−	−
6h	+	+	**7b**	−	−
6i	−	+	**7c**	−	−
6j	+	+	**7d**	−	−
6k	+	+	NSC-663284	+	−
6l	+	+	4-amino-1-naphthol	+	+
6m	−	+	Fluconazole	−	−
6n	+	+			

Table S1 | Redox-activity of select compounds in Rtt109 HTS-like conditions. Selected compounds were tested for the ability to generate H_2O_2 in HTS buffer in the presence and absence of DTT using a surrogate HRP-PR assay. Compounds were flagged as redox-positive if they showed greater than 2X background signal (DMSO) at final compound concentrations between 10-125 μM and evidence of dose-response. NSC-663284, 4-amino-1-naphthol and fluconazole were included as control compounds.

HAT	DTT	Percent inhibition		
		1 mM H_2O_2	250 µM H_2O_2	62.5 µM H_2O_2
Rtt109-Vps75	+	20 ± 10	3 ± 3	0 ± 10
	−	20 ± 5	15 ± 4	3 ± 7
p300-BHC	+	12 ± 5	2 ± 2	-1 ± 3
	−	54 ± 10	35 ± 10	13 ± 8
Gcn5-Ada2-Ada3	+	22 ± 10	12 ± 10	17 ± 10
	−	8 ± 8	8 ± 9	10 ± 10

Table S2 | Sensitivities of *in vitro* HAT assays to H_2O_2. Rtt109-Vps75, p300-BHC and Gcn5-Ada2-Ada3 were incubated with H_2O_2 under HTS-like assay conditions in either the presence or absence of the reducing agent DTT (1 mM final concentration). Percent inhibition of enzymatic activity was calculated as a percentage of DMSO controls. Percent inhibition values shown are means ± SD for three replicates.

Cpd	Protein	Peptide adduct detected	Key fragment ions	PEAKS peptide score[a] (-10 logP)	Precursor mass error (ppm)
1a	Rtt109	LIFVSKADTNGY**C**(+163.99)NTR	y^4 through y^{12}	58	0.5
		FQQDLYLSFT**C**(+163.99)PR	y^3 through y^9	45	2.9
		I**C**(+163.99)LFTRPASQYLFPDSSK	b^2 through b^6	60	0.4
	Vps75	**C**(+163.99)EEEVDAIER	b^2 through b^4	65	-1.3
		EFPHGDSLASLFSEEIYPF**C**(+163.99)VK	y^3 through y^6	66	2.4
	Asf1	S**C**(+163.99)SYDGR	b^2 through b^3	36	1.7
6a	Rtt109	ADTNGY**C**(+172.02)NTR ADTNGY**C**(+156.02)NTR	y^4 through y^8	54	-1.4
			y^4 through y^8	54	0.8
	Vps75	AFLGLAK**C**(+172.02)EEEVDAIER	y^{10} through y^{12}	76	-4.8
	Asf1	None	–	–	–
6b	Rtt109	ADTNGY**C**(+172.02)NTR	y^4 through y^7	43	0.4
	Vps75	AFLGLAK**C**(+172.02)EEEVDAIER	y^{10} through y^{11}	84	-3.2
		EFPHGDSLASLFSEEIYPF**C**(+156.02)VK	y^3 through y^6	49	3.9
	Asf1	None	–	–	–
CPM	Rtt109	ADTNGY**C**(+402.16)NTR	y^4 through y^6	47	4.8
	Vps75	**C**(+402.16)EEEVDAIER	b^2 through b^3	64	4.2
	Asf1	None	–	–	–

[a] Score derived from the *p*-value that indicates the statistical significance of the peptide-spectrum match. Good quality score > 25 – 45; high quality score > 45[1].

Table S3 | Compound-peptide adducts detected by protein mass spectrometry. Compounds **1a, 6a and 6b** were incubated with yeast Rtt109, Vps75 or Asf1. CPM was included as a positive thiol-reactive control compound. Representative, high-confidence peptide adducts are provided. Support for detection of compound-peptide adducts from tandem MS data is based on: (1) very high confidence in the peptide sequence from fragment ions that support at least five consecutive b- or y-type fragment ions; (2) expected mass accuracy for precursor *m/z* (< 7 ppm); and (3) key peaks that support site localization of cysteine modification on amino acid fragments.

Chemotype -subtype	Query[a]	N	N_{data}[b]	N (pBSF > 2)	Fraction (%)[c]
1-ii	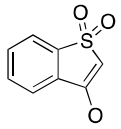	5	5	0	0.0
1-iii	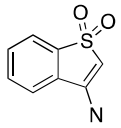	29	25	1	4.0
1-iv	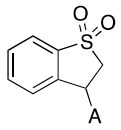	52	42	2	4.7
2-iii	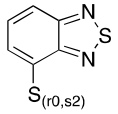	3	3	2	66.7
2-iv	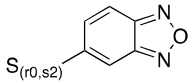	2	2	1	50.0
3-ii	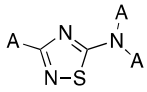	971	910	12	1.3
3-iii	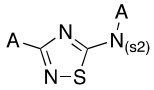	760	629	61	9.7
3-iv	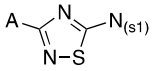	104	67	5	7.5
3-v	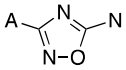	243	168	6	3.6
4-ii	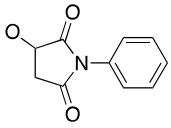	13	12	0	0.0
4-iii	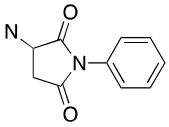	804	753	17	2.3
6-ii	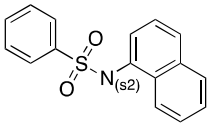	230	209	85	40.7
6-iii	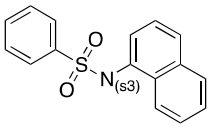	32	24	3	12.5
6-iv	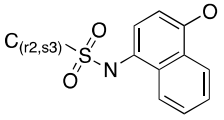	118	112	72	64.3

7-**iii**	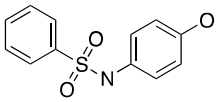	3157	2,446	321	13.1
7-**iv**	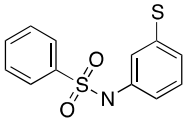	166	134	18	13.4

[a] Structure annotations: A, any atom; *n*s, number of substituents (e.g. "2s"); *n*r number of connected ring bonds (e.g. "2r"); X, halogen.
[b] N_{data} designates the subset of compounds for which a pBSF score had been derived. This is dependent on the availability of HTS screening data.
[c] Expected incidence of anomalous binders is 6% (averaged over all compounds).

Table S4 | Additional analysis of thiol-reactive chemotype bioassay promiscuity in an industrial HTS setting. See also Table 7.

Structure	Reported biological target and mechanism of action	Reference
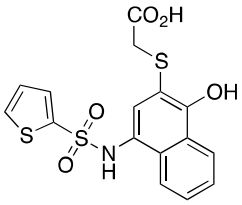	Chymotrypsin-like activity of proteasome inhibitor	2
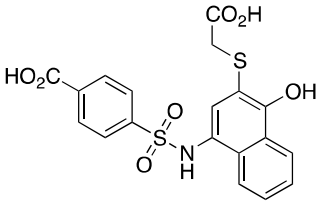	Stat3 inhibitor	3
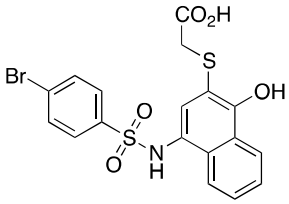	Mcl-1 inhibitor	4
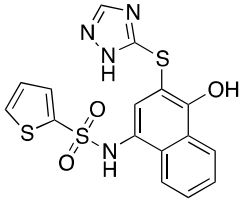	$BRAF^{V600E}$ inhibitor	5

Table S5 | Published examples of compounds containing chemotype 6 that are unlikely to be selective chemical probes.

CHEMICAL SYNTHESES AND CHARACTERIZATION

General description

The ^{1}H NMR (400 MHz) and ^{13}C NMR (100 MHz) spectra were recorded on a Bruker Avance spectrometer. The ^{13}C NMR (176 MHz) spectra were recorded on a Bruker Avance III 700-MHz spectrometer with a 1.7-mm TCI Cryoprobe. Chemical shifts are reported in ppm using the solvent peak as an internal standard. Data are reported as follows: chemical shift, multiplicity (s = singlet, brs = broad singlet, d = doublet, t = triple, q = quartet, m = multiplet), coupling constant, and integration.

Samples were analyzed for purity using a Waters Acquity UPLC system equipped with a BEH C18 2.1 x 50 mm column. The flow rate was 0.250 mL/min with a standard gradient starting at 95% Solution A (950 mL H_2O, 50 mL MeCN, 1 mL formic acid) and ending with 100% Solution B (1000 mL MeCN plus 1 mL formic acid) over 6.5 min. The samples were monitored simultaneously using an ELS detector, a diode array detector (214, 220, 244 and 254 nm) and a ZQ mass spectrometer (ESI positive and negative ion modes). Low-resolution mass spectra (LRMS) were recorded using this ZQ mass spectrometer.

High-resolution mass spectra (HRMS) were recorded as previously described[6]. The instrumentation consisted of a Waters Acquity UPLC equipped with a Waters HSS T3 C18 2.1 mm x 100 mm column (1.7 mm diameter particles) coupled to a Waters Synapt G2 HDMS quadrupole orthogonal acceleration time of flight mass spectrometer. The solvents consisted of Solution A (H_2O containing 0.1% formic acid) and Solution B (MeCN containing 0.1% formic acid). The flow rate was 0.400 mL/min with a 26 min linear gradient separation at 35 °C as follows: 3% B, 0 min to 5 min; 3% B to 97% B, 5 min to 18 min; 97% B, 18 min to 21 min; 97% B to 3% B, 21 min to 23 min; 3% B 23 min to 26 min. Mass spectra were collected from *m/z* 50-1200 every 100 ms during the chromatographic separation. On-the-fly mass calibration was performed using an infusion of a leucine-enkephalin solution.

Screening compound characterization

4-(5-((1,1-Dioxidobenzo[*b*]thiophen-3-yl)thio)-1*H*-tetrazol-1-yl)benzoic acid (**1a**). ^{1}H NMR (400 MHz, DMSO-d_6) δ 13.43 (brs, 1H), 8.18−8.20 (m, 2H), 7.92−7.95 (m, 3H), 7.65−7.77 (m, 3H), 7.46 (1H, s). ^{13}C NMR (100 MHz, DMSO-d_6) δ 166.1, 147.8, 138.0, 136.3, 136.1, 134.3, 133.1, 132.0, 130.8, 129.0, 127.2, 125.4, 123.0, 121.3. UPLC: purity 99% (ELS), rt = 4.14 min. LRMS (ESI+): 387 [M + H].

4-((9*H*-Purin-6-yl)thio)-7-bromo-5-nitrobenzo[*c*][1,2,5]thiadiazole (**2a**). ^{1}H NMR (400 MHz, DMSO-d_6) δ 13.69 (s, 1H), 8.77 (s, 1H), 8.46 (s, 1H), 8.44 (s, 1H). ^{13}C NMR (100 MHz, DMSO-d_6) δ 155.0, 153.4, 153.0, 152.9, 151.3, 150.7, 144.5, 130.2, 127.1, 117.9, 116.3. UPLC: purity 97% (ELS), rt = 4.09 min. LRMS (ESI+): 410, 412 [M + H + H_2O].

5-(Methylamino)-2,3-diphenyl-1,2,4-thiadiazol-2-ium bromide (**3a**). ^{1}H NMR (400 MHz, CD_3OD) δ 7.49−7.62 (m, 9H), 7.38−7.42 (m, 2H), 3.38 (s, 3H). ^{13}C NMR (100 MHz, CD_3OD) δ 178.4, 168.9, 136.0, 134.2, 132.3, 131.8, 131.8, 131.7, 131.6, 129.9, 129.8, 128.7, 128.6, 127.9, 32.1. UPLC: purity 99% (ELS), rt = 3.33 min. LRMS (ESI+): 268 [M + H].

1-(4-Bromophenyl)-3-((5-(2-hydroxyphenyl)-1,3,4-oxadiazol-2-yl)thio)pyrrolidine-2,5-dione (**4a**). ^{1}H NMR (400 MHz, acetone-d_6) δ 9.74 (s, 1H), 7.79 (d, *J* = 7.9 Hz, 1H), 7.71 (d, *J* = 8.4 Hz, 2H), 7.53 (dd, *J* = 8.5, 7.3 Hz, 1H), 7.36 (d, *J* = 8.4 Hz, 2H), 7.03−7.15 (m, 2H), 5.09 (dd, *J* = 9.7, 5.4 Hz, 1H), 3.65 (dd, *J* = 18.4, 9.4 Hz, 1H), 3.32 (dd, *J* = 18.5, 5.4 Hz, 1H). ^{13}C NMR (167 MHz, acetone-d_6) δ 173.9, 173.7, 166.5, 162.3, 157.9, 134.8, 133.1, 132.9, 129.8, 127.8, 122.6, 121.1, 118.1, 108.9, 43.2, 36.8. UPLC: purity 95% (ELS), rt = 5.21 min. LRMS (ESI+): 446, 448 [M + H].

3-((4-((4-Bromophenyl)sulfonamido)-1-hydroxynaphthalen-2-yl)thio)propanoic acid (**6a**). ^{1}H NMR (400 MHz, CD_3OD) δ 8.21−8.23 (m, 1H), 7.89−7.91 (m, 1H), 7.61−7.64 (m, 2H), 7.55−7.57 (m, 2H), 7.43−7.47 (m, 2H), 7.08 (s, 1H), 2.89 (t, *J* = 7.2 Hz, 2H), 2.46 (t, *J* = 7.2 Hz, 2H). ^{13}C NMR (100 MHz, CD_3OD) δ 175.4, 155.6, 140.4, 133.6, 133.3, 132.5, 130.3, 128.4, 128.3, 126.9, 126.3, 125.2, 124.3, 124.1, 112.0, 35.1, 32.0. UPLC: purity 96% (ELS), rt = 4.74 min. LRMS (ESI+): 499, 501 [M + H + H_2O].

***N*-(3-((1*H*-1,2,4-Triazol-3-yl)thio)-4-hydroxynaphthalen-1-yl)naphthalene-2-sulfonamide** (**6b**). ^{1}H NMR (400 MHz, CD_3OD) δ 8.2−8.24 (m, 1H), 8.13−8.15 (m, 2H), 7.96 (d, *J* = 8.1 Hz, 1H), 7.88−7.92 (m, 2H), 7.84 (d, *J* = 8.1 Hz, 1H), 7.71 (dd, *J* = 8.7, 1.8 Hz, 1H), 7.57 (m, 1H), 7.63 (m, 1H), 7.35-7.45 (m, 2H), 6.99 (s, 1H).^{13}C NMR (100 MHz, CD_3OD) δ 155.5, 138.1, 136.2, 134.1, 133.4, 131.5, 130.2, 130.2, 129.8, 129.6, 128.9, 128.5, 128.5, 127.3, 127.0, 126.1, 124.5, 124.0, 123.8. UPLC: purity 97% (ELS), rt = 4.39 min. LRMS (ESI+): 449 [M + H].

Compound-GSH adduct syntheses and characterization

***N*^{5}-((*R*)-1-((Carboxymethyl)amino)-3-((1,1-dioxidobenzo[*b*]thiophen-3-yl)thio)-1-oxopropan-2-yl)-*L*-glutamine** (**1a'**). 4-(5-((1,1-Dioxidobenzo[*b*]thiophen-3-yl)thio)-1*H*-tetrazol-1-yl)benzoic acid **1a** (2 mg, 5.18 µmol) was dissolved in MeCN (0.8 mL), H_2O (2.2 mL) and HTS buffer (0.2 mL). This mixture was shaken at 30 °C for 5 min, then GSH (3.2 mg, 10.41 µmol) was added. The reaction was shaken at 30 °C and monitored by UPLC-MS until starting material was consumed. The crude reaction analyzed by LC-HRMS for the titled compound **1a'**: rt = 8.00 min. HRMS (ES+) *m/z* calculated for $C_{18}H_{22}N_3O_8S_2^+$ [M + H], 472.0843; found, 472.0857 (error 3.0 ppm).

***N*^{5}-((*R*)-3-((7-Bromo-5-nitrobenzo[*c*][1,2,5]thiadiazol-4-yl)thio)-1-((carboxymethyl)amino)-1-oxopropan-2-yl)-*L*-glutamine** (**2a'**). 4-((9*H*-Purin-6-yl)thio)-7-bromo-5-nitrobenzo[*c*][1,2,5]thiadiazole **2a** (2 mg, 4.88 µmol) was dissolved in MeCN (0.8 mL), H_2O (2 mL) and HTS buffer (0.195 mL). This mixture was shaken at 30 °C for 5 min, then GSH (3.0 mg, 9.75 µmol) was added. The reaction was shaken at 30 °C and monitored by UPLC-MS until starting material was consumed. The crude reaction analyzed by LC-HRMS for the titled compound **2a'**: rt = 9.24 min. HRMS (ES+) *m/z* calculated for $C_{16}H_{18}BrN_6O_8S_2^+$ [M + H], 564.9805; found, 564.9828 (error 4.1 ppm).

(*Z*)-*N*-Methyl-*N*'-((*E*)-phenyl(phenylimino)methyl)carbamimidothioic acid (**3a''**). 5-(Methylamino)-2,3-diphenyl-1,2,4-thiadiazol-2-ium bromide **3a** (2 mg, 5.74 µmol) was dissolved in MeCN (0.68 mL), H_2O (2.4 mL), and HTS buffer (0.23 mL). This mixture was shaken at 30 °C for 5 min, then GSH (3.5 mg, 11 µmol) was added. The reaction was shaken at 30 °C and monitored by UPLC-MS until starting material was consumed. The crude reaction analyzed by LC-HRMS for the titled compound **3a''**: rt = 13.07 min. HRMS (ES+) *m/z* calculated for $C_{15}H_{16}N_3S^+$ [M + H], 270.1059; found, 270.1072 (error 4.8 ppm).

***N*^{5}-((2*R*)-3-((1-(4-bromophenyl)-2,5-dioxopyrrolidin-3-yl)thio)-1-((carboxymethyl)amino)-1-oxopropan-2-yl)-*L*-glutamine** (**4a'**). 1-(4-bromophenyl)-3-((5-(2-hydroxyphenyl)-1,3,4-oxadiazol-2-yl)thio)pyrrolidine-2,5-dione **4a** (1 mg, 2.241 µmol) was dissolved in MeCN (0.2 mL) and HTS buffer (4.5 mL). This mixture was shaken at 30 °C for 5 min, then GSH (1.4 mg, 4.56 µmol) was added. The reaction was shaken at 30 °C and monitored by UPLC-MS until starting material was consumed. The crude reaction analyzed by LC-HRMS for the titled compound **4a'**: rt = 8.98 min. HRMS (ES+) *m/z* calculated for $C_{20}H_{26}BrN_4O_9S^+$ [M + H + H_2O], 577.0598, 579.0578; found, 577.0605, 579.0588 (error 1.2 ppm).

***N*^{5}-((*R*)-1-((Carboxymethyl)amino)-3-((1,4-dioxo-1,4-dihydronaphthalen-2-yl)thio)-1-oxopropan-2-yl)-*L*-glutamine** (**6''**). 3-((4-((4-Bromophenyl)sulfonamido)-1-hydroxynaphthalen-2-yl)thio)propanoic acid **6a** (10.8 mg, 22 µmol) was dissolved in MeCN (5 mL), H_2O (9 mL), and HTS buffer (10 mL). This mixture was shaken at 30 °C for 5 min, then GSH (13.8 mg, 44.9 µmol) was added. The reaction was shaken at 30 °C and monitored by UPLC-MS until starting material was consumed. The crude reaction analyzed by LC-HRMS for the titled compound **6''**: rt = 8.62 min. HRMS (ES+) *m/z* calculated for $C_{20}H_{22}N_3O_8S^+$ [M + H], 464.1122; found, 464.1139 (error 3.7 ppm).

***N*^{5}-((*R*)-1-((Carboxymethyl)amino)-3-((1,4-dioxo-1,4-dihydronaphthalen-2-yl)thio)-1-oxopropan-2-yl)-*L*-glutamine** (**6''**). *N*-(3-((1*H*-1,2,4-triazol-3-yl)thio)-4-hydroxynaphthalen-1-yl)naphthalene-2-sulfonamide **6b** (2.9 mg, 6.47 µmol) was dissolved in MeCN (2.3 mL), H_2O (3 mL), and HTS buffer (5 mL). This mixture was shaken at 30 °C for 5 min, then GSH (4 mg, 13 µmol) was added. The reaction was shaken at 30 °C and monitored by UPLC-MS until starting material was consumed. The crude reaction analyzed by LC-HRMS for the titled compound **6''**: rt = 8.63 min. HRMS (ES+) *m/z* calculated for $C_{20}H_{22}N_3O_8S^+$ [M + H], 464.1122; found, 464.1135 (error 2.8 ppm).

^{1}H NMR, compound **1a**

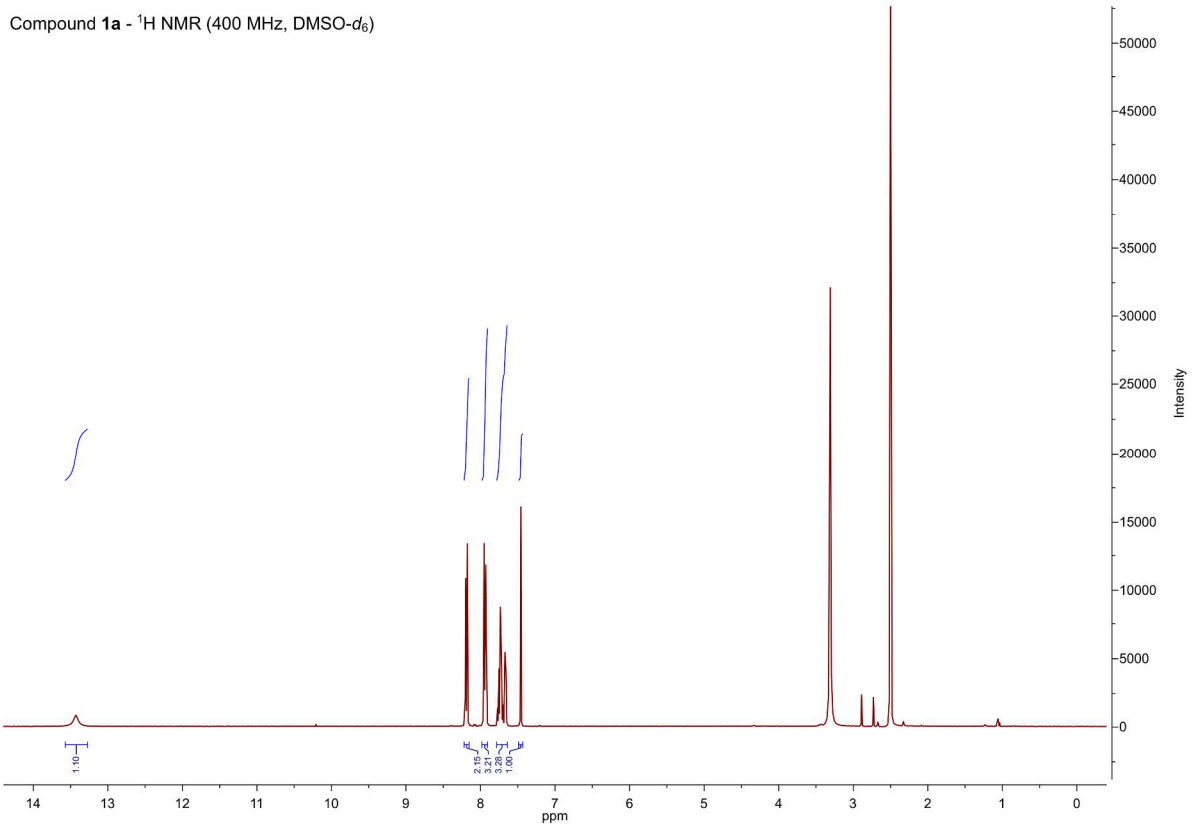

^{13}C NMR, compound **1a**

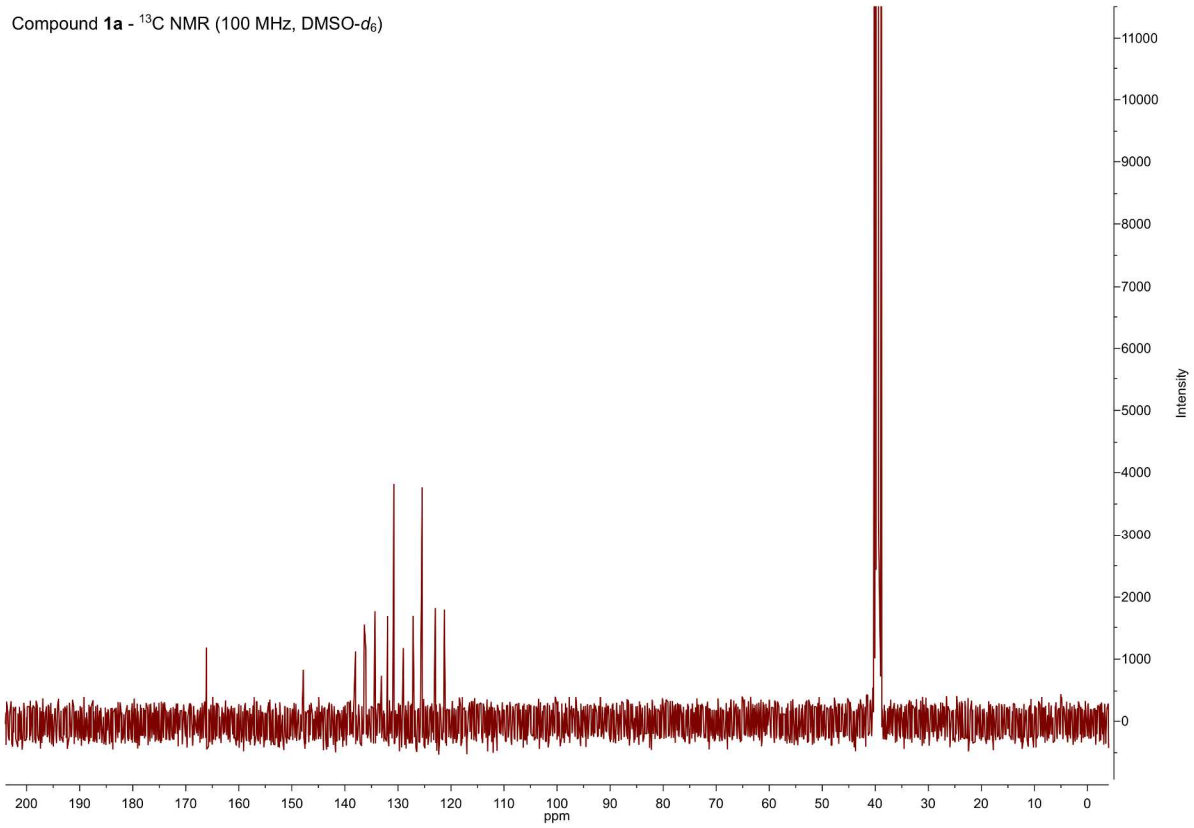

UPLC-MS, compound **1a**

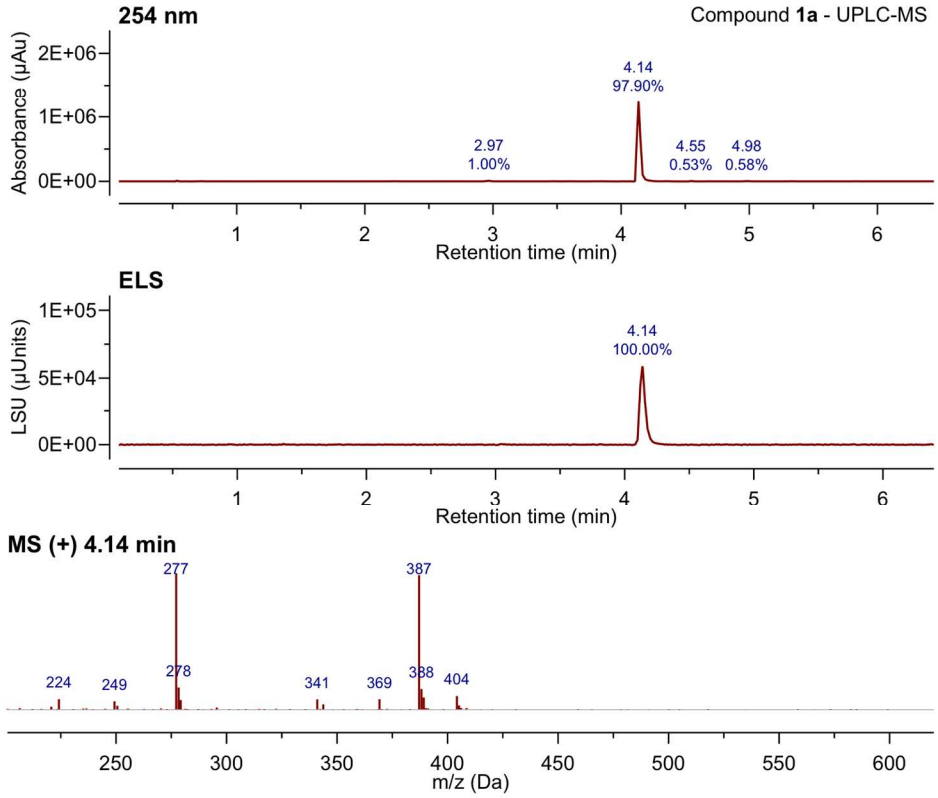

^{1}H NMR, compound **2a**

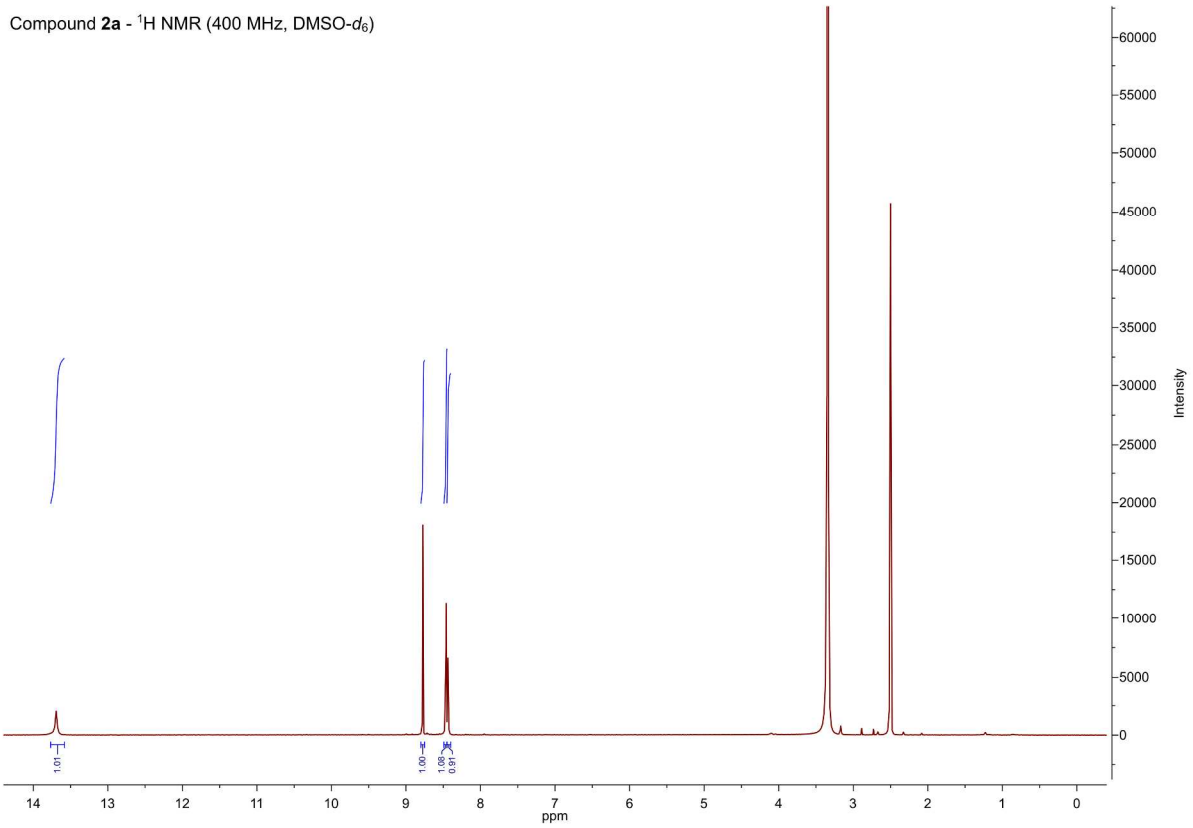

^{13}C NMR, compound **2a**

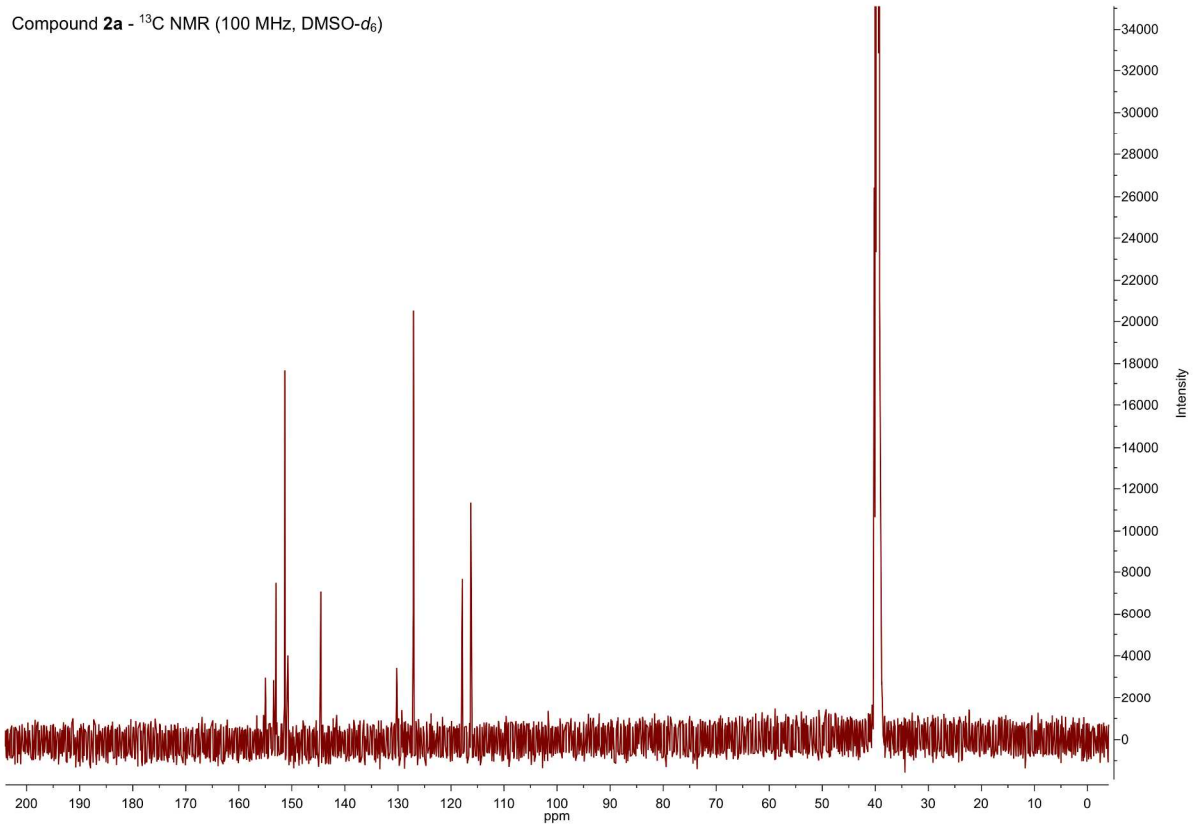

UPLC-MS, compound **2a**

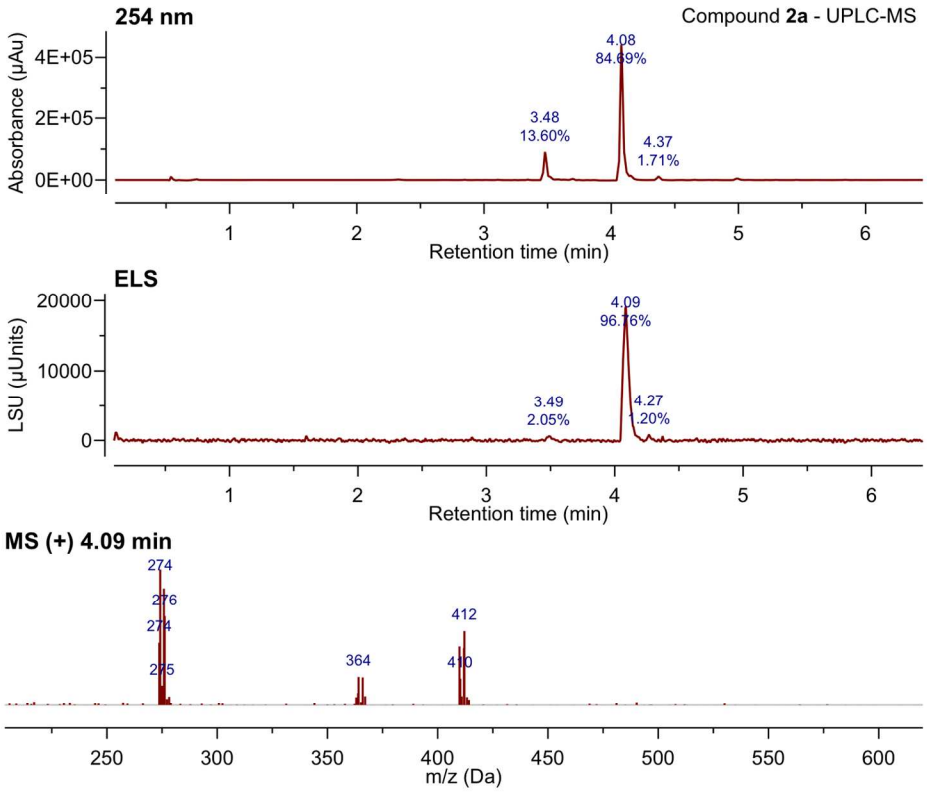

^{1}H NMR, compound **3a**

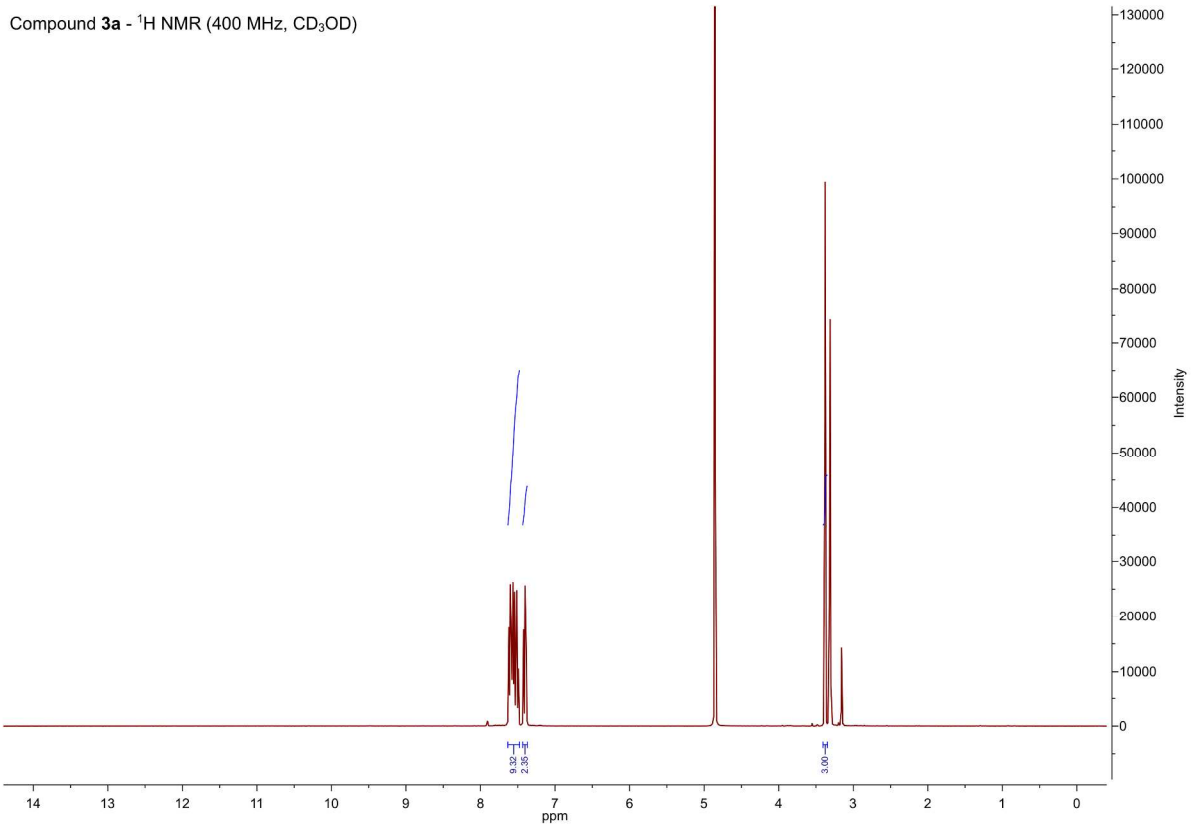

^{13}C NMR, compound **3a**

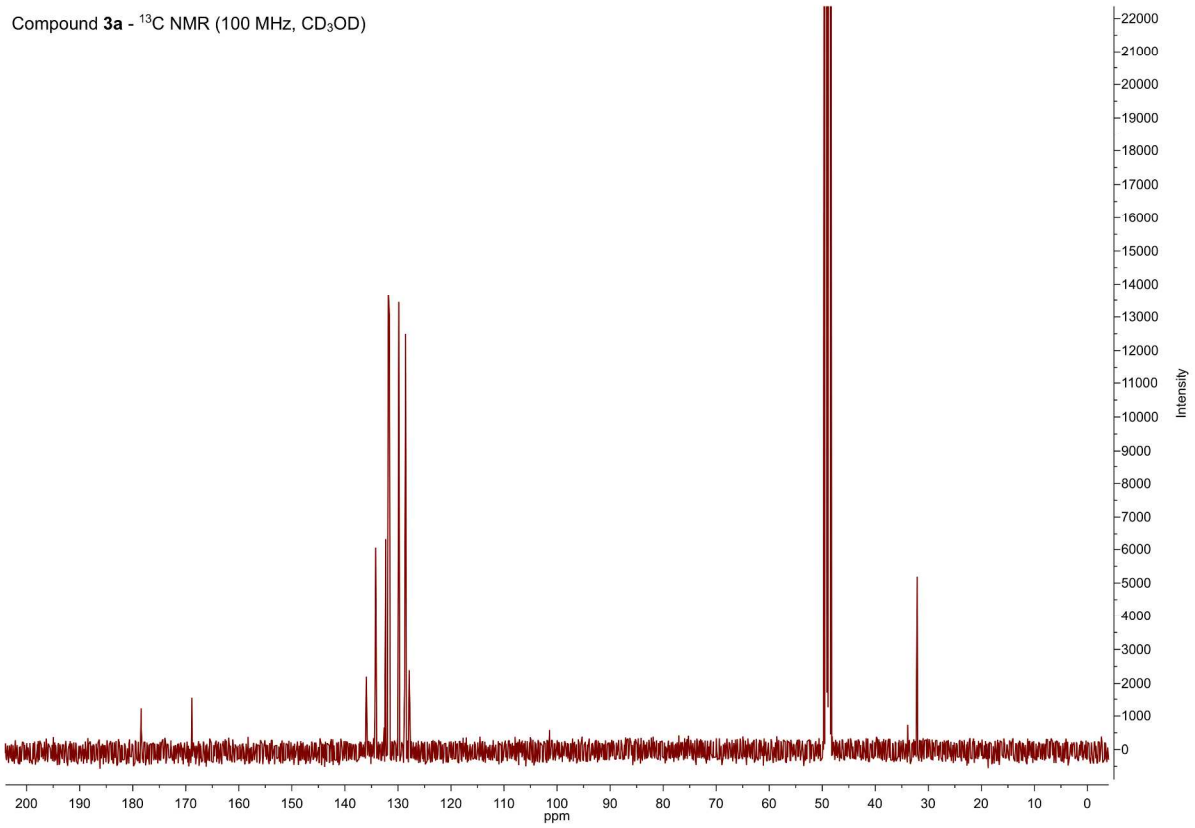

UPLC-MS, compound **3a**

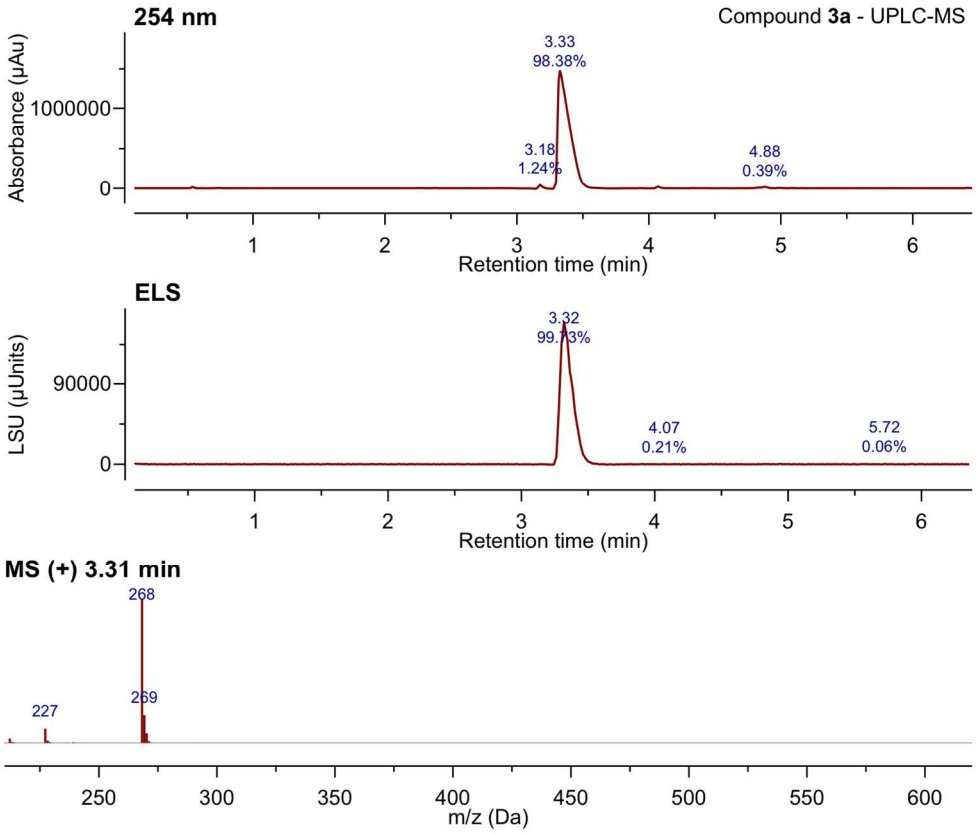

^{1}H NMR, compound **4a**

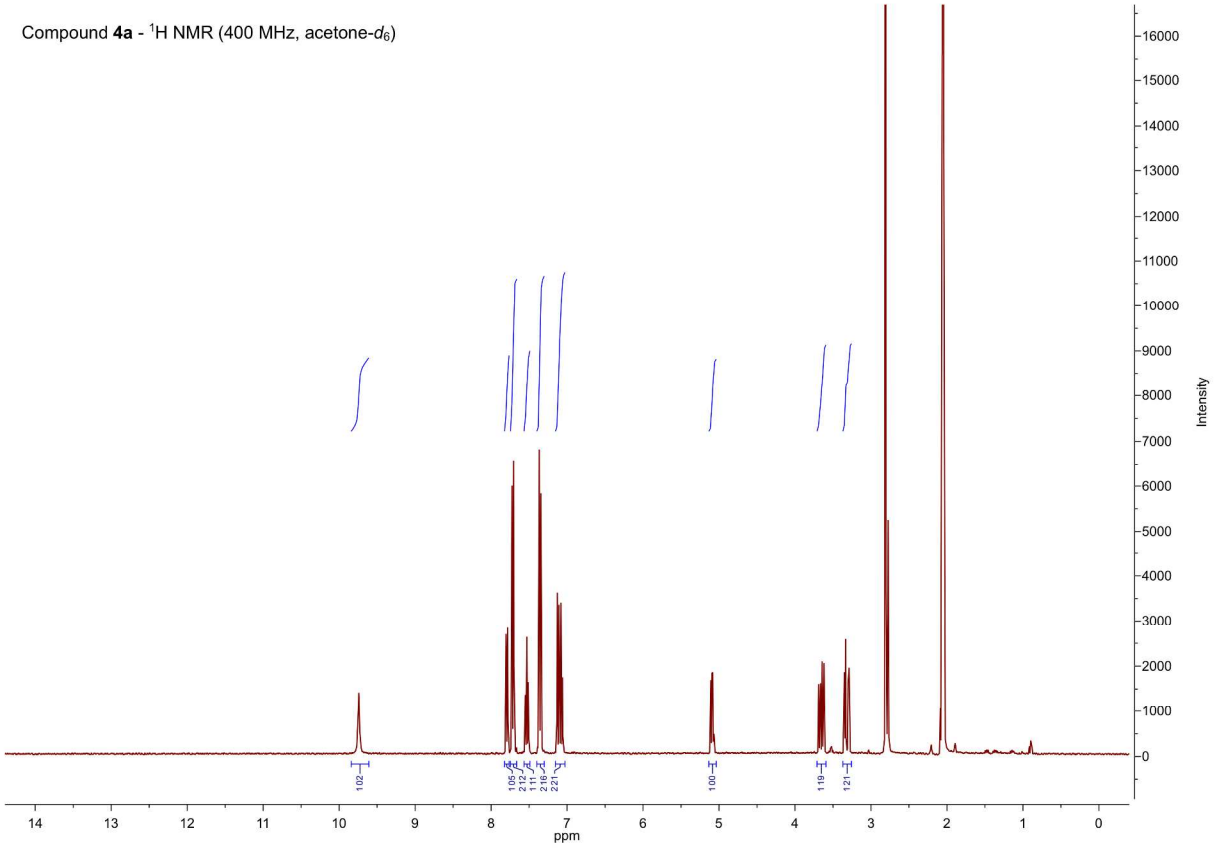

^{13}C NMR, compound **4a**

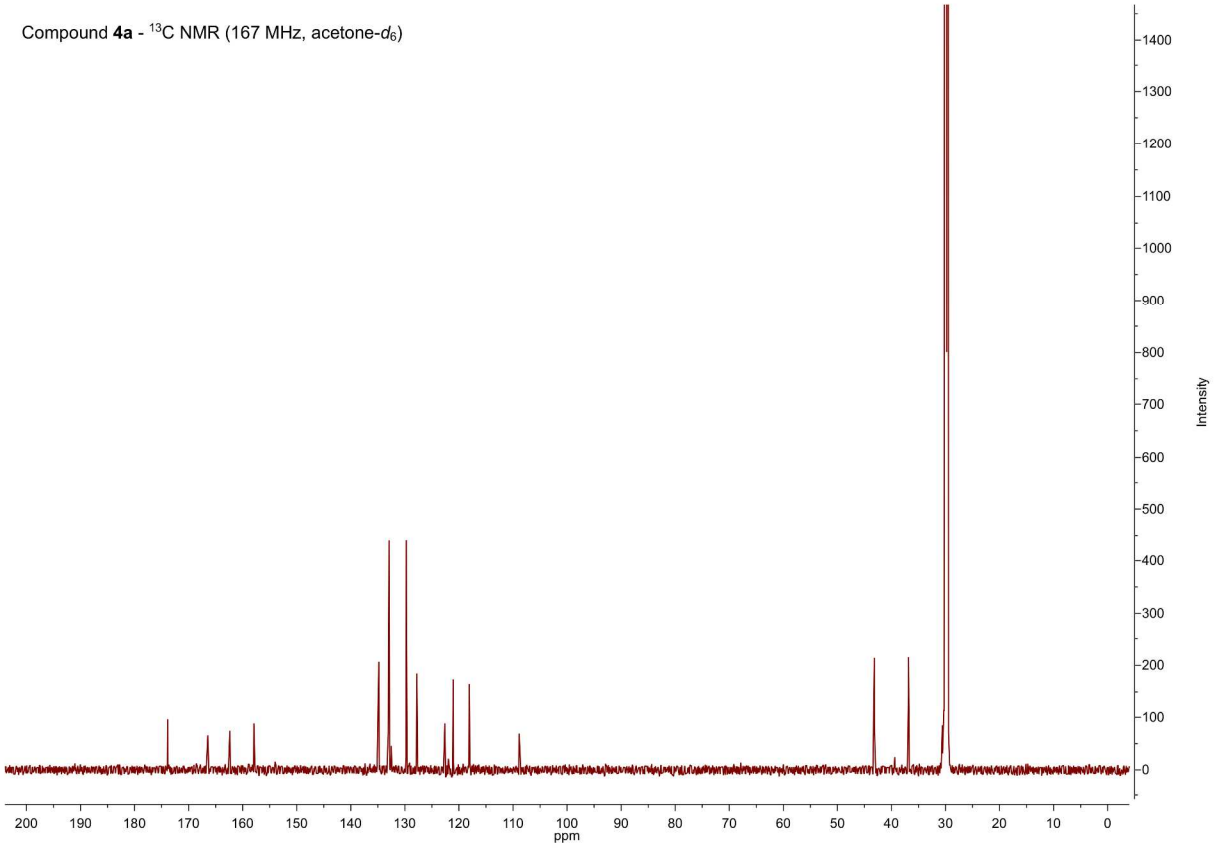

UPLC-MS, compound **4a**

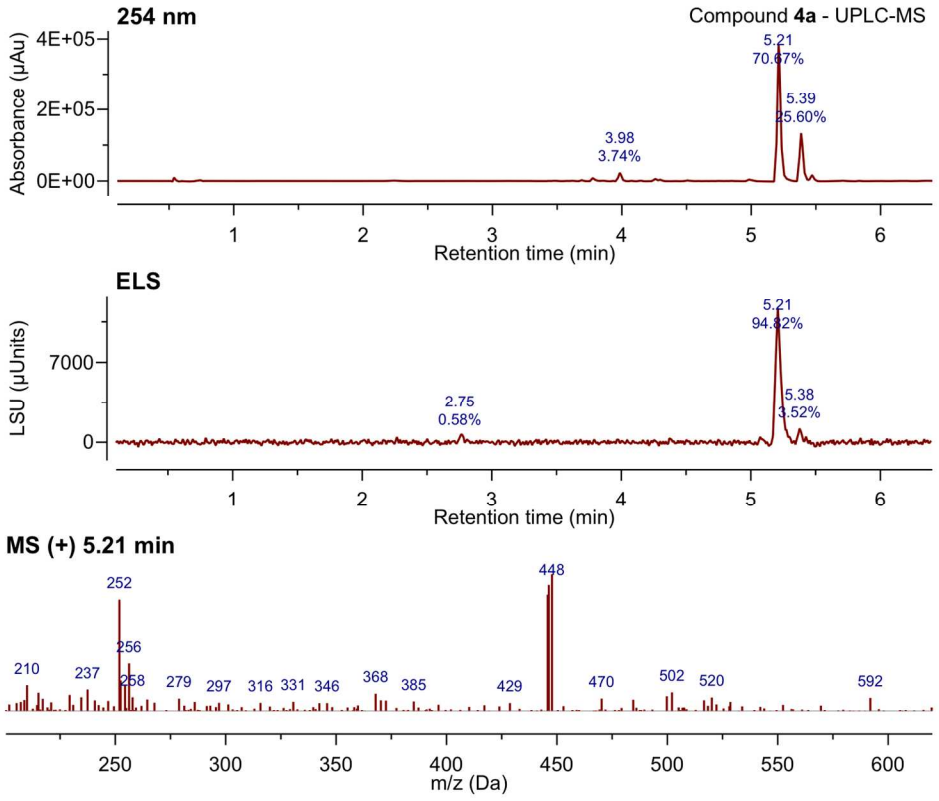

^{1}H NMR, compound **6a**

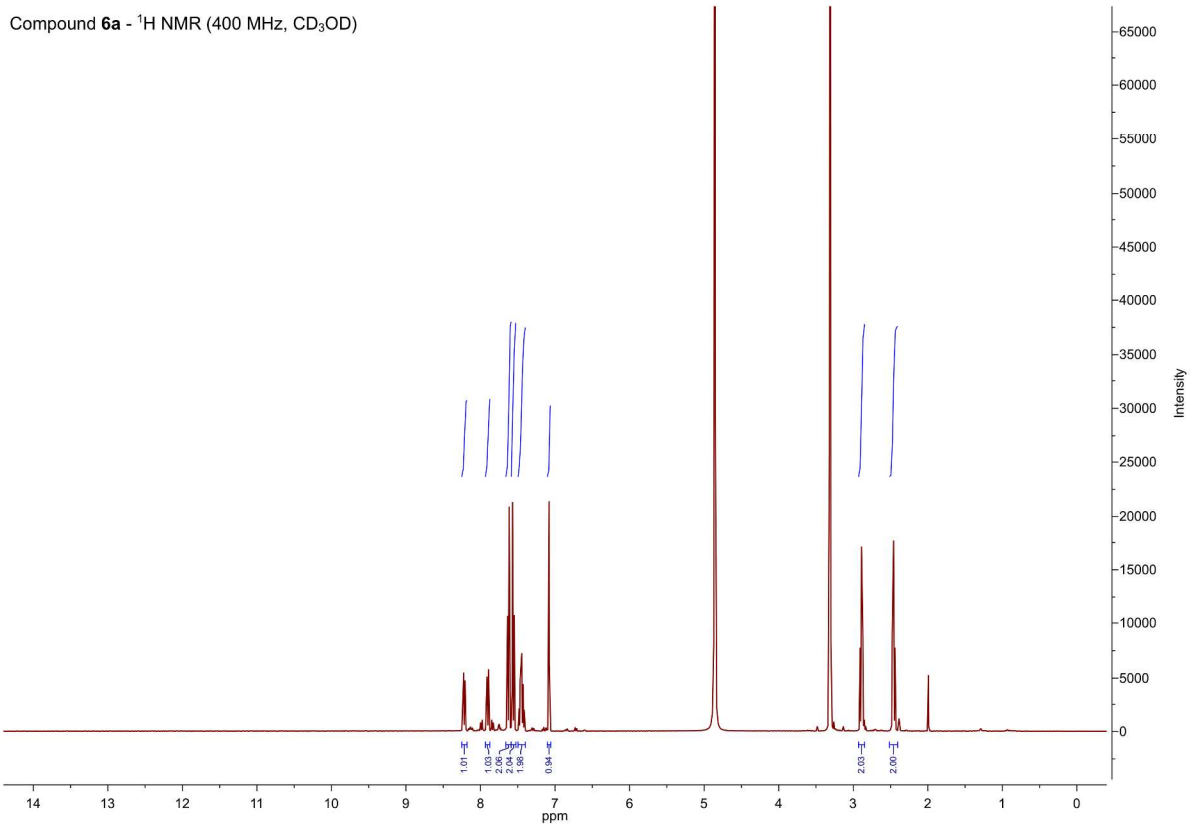

^{13}C NMR, compound **6a**

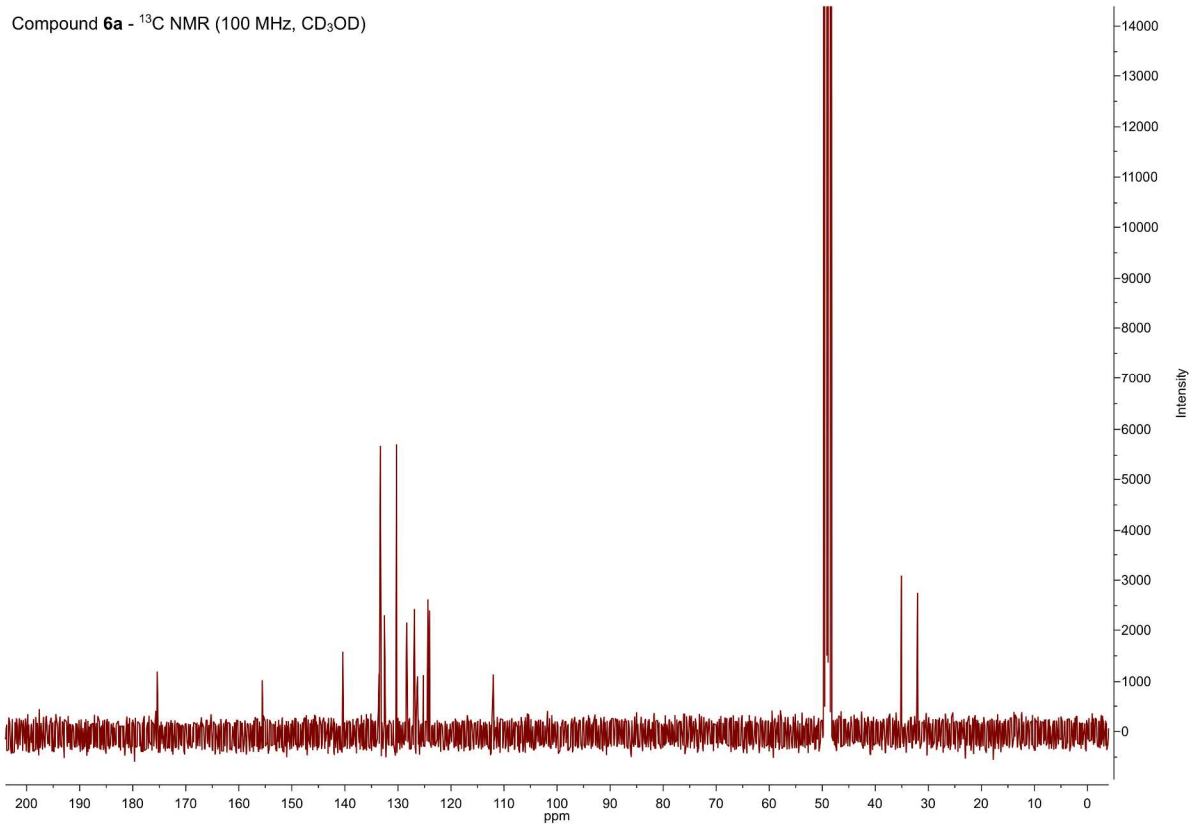

UPLC-MS, compound **6a**

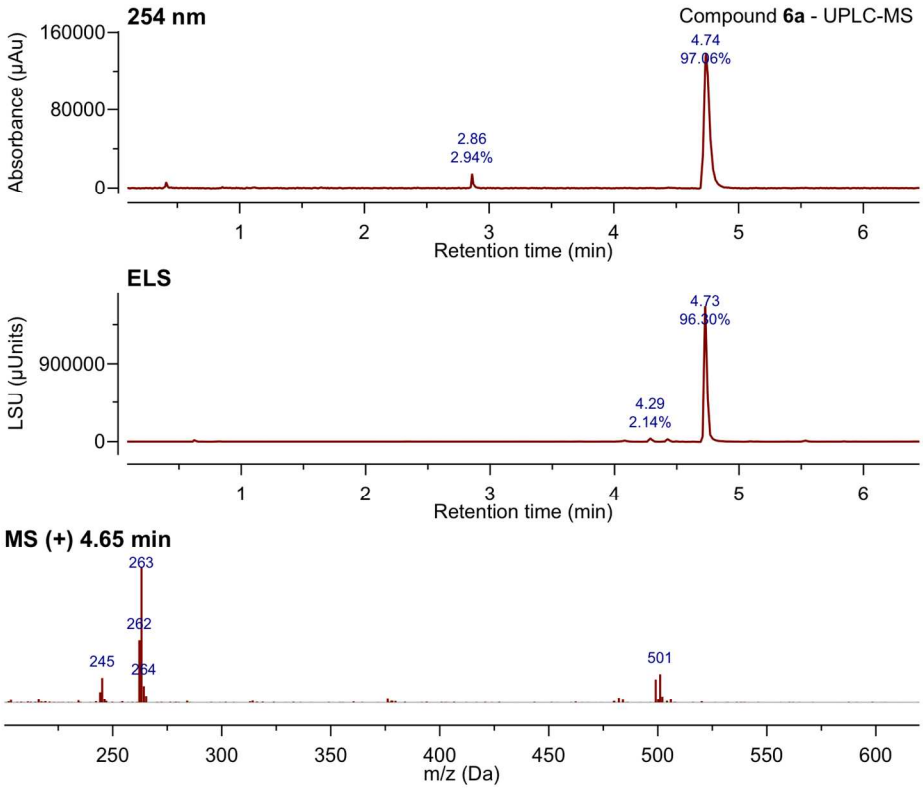

^{1}H NMR, compound **6b**

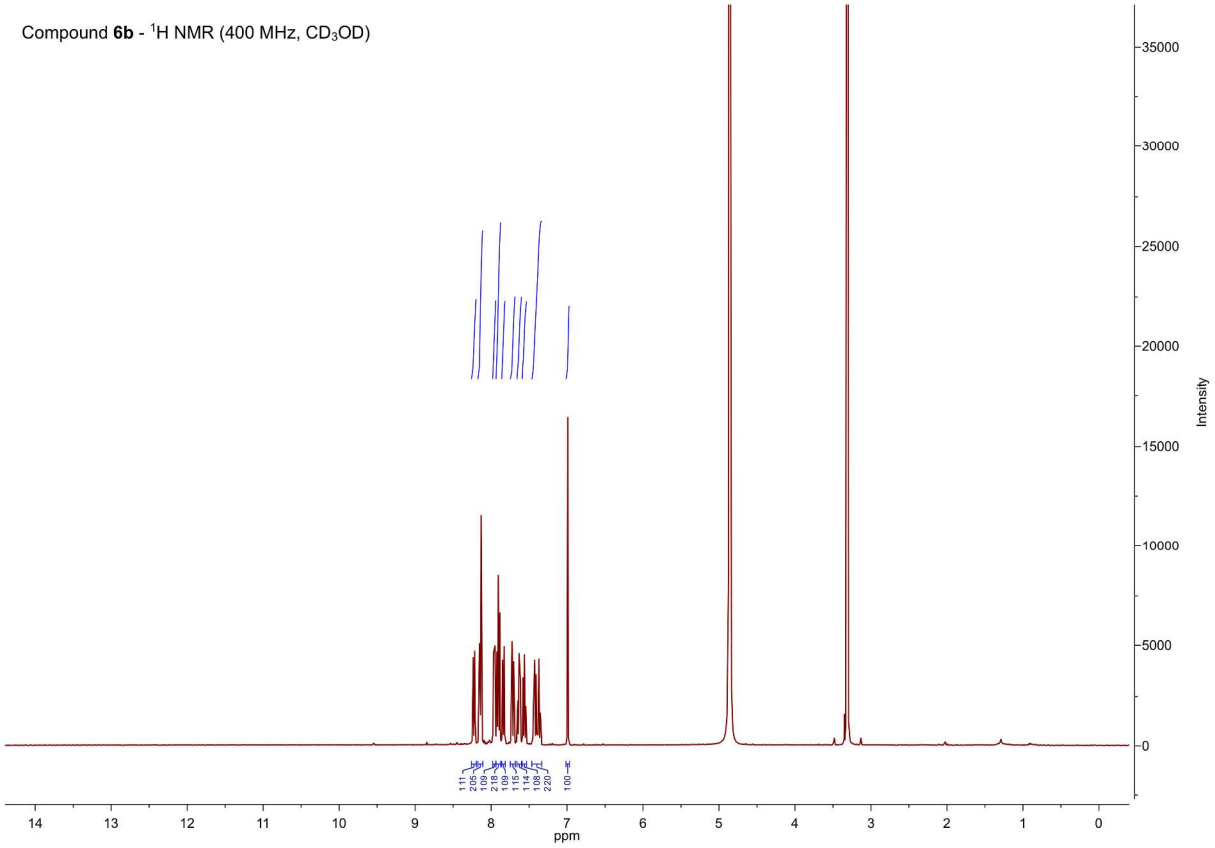

^{13}C NMR, compound **6b**

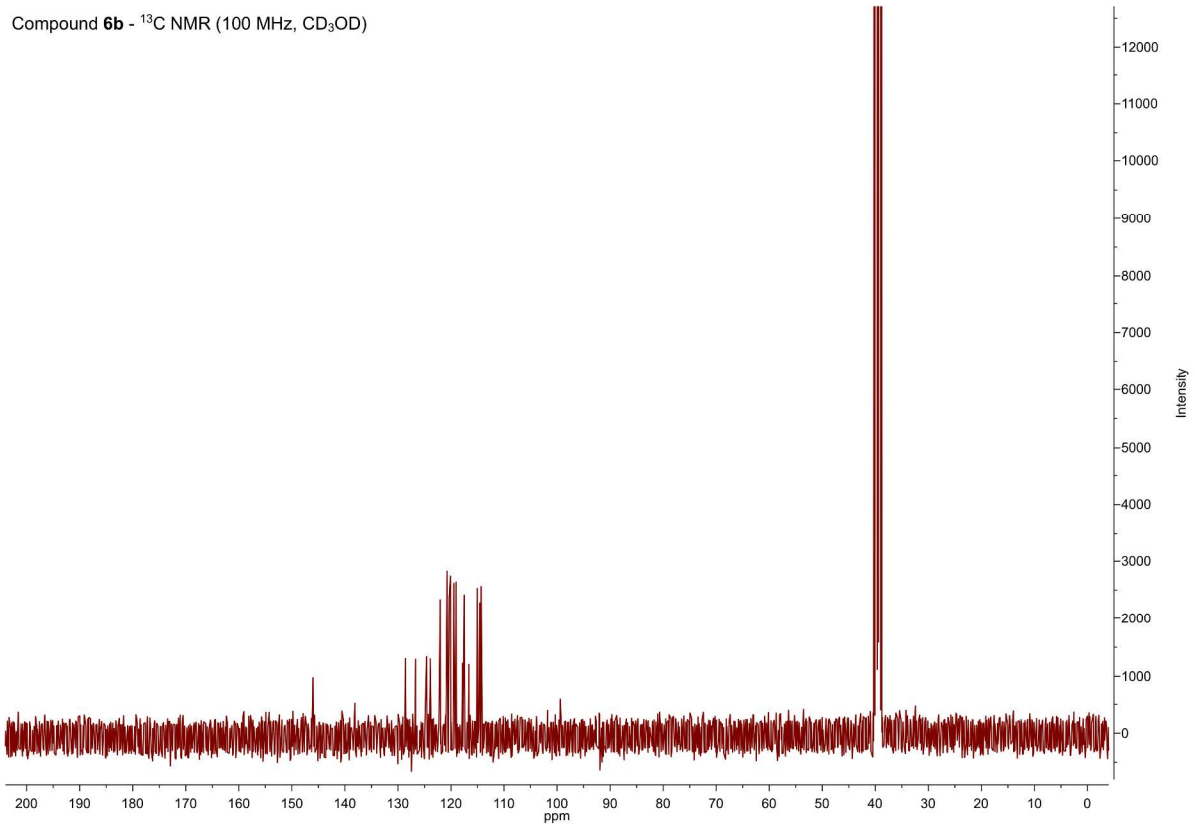

UPLC-MS, compound **6b**

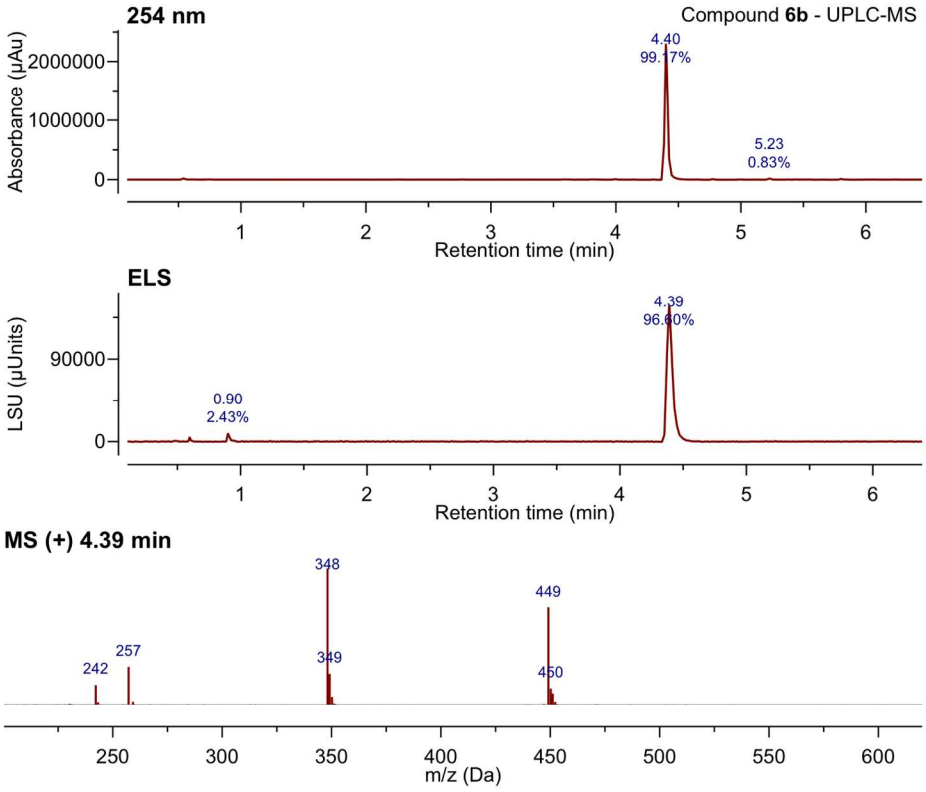

LC-HRMS, adduct **1a'** (via **1a** + GSH in HTS buffer)

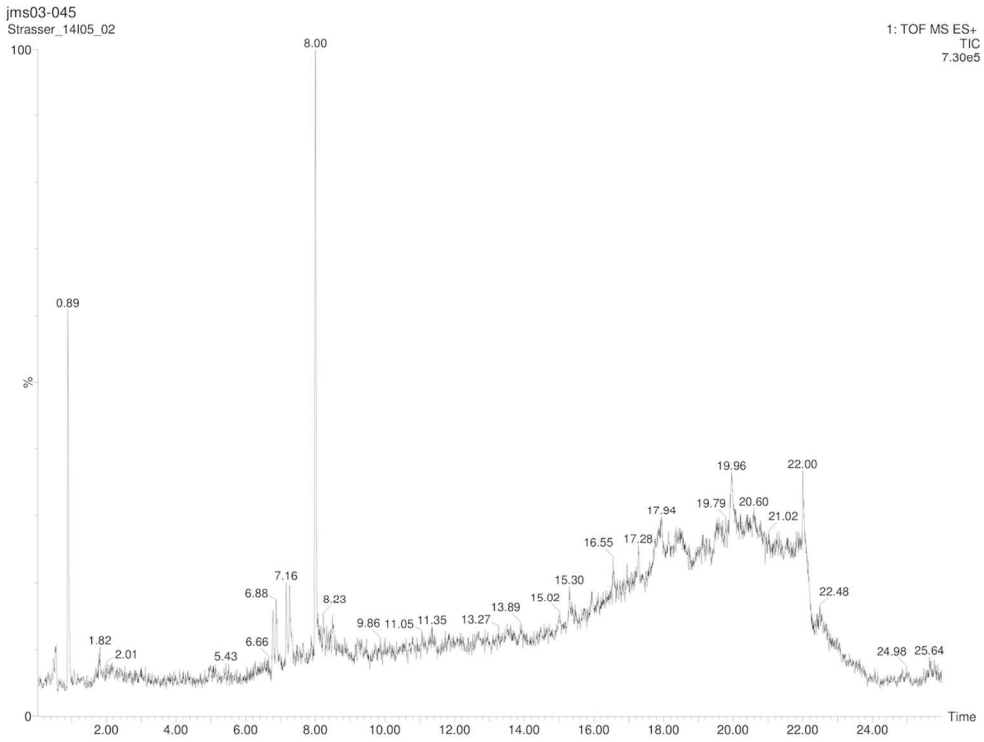

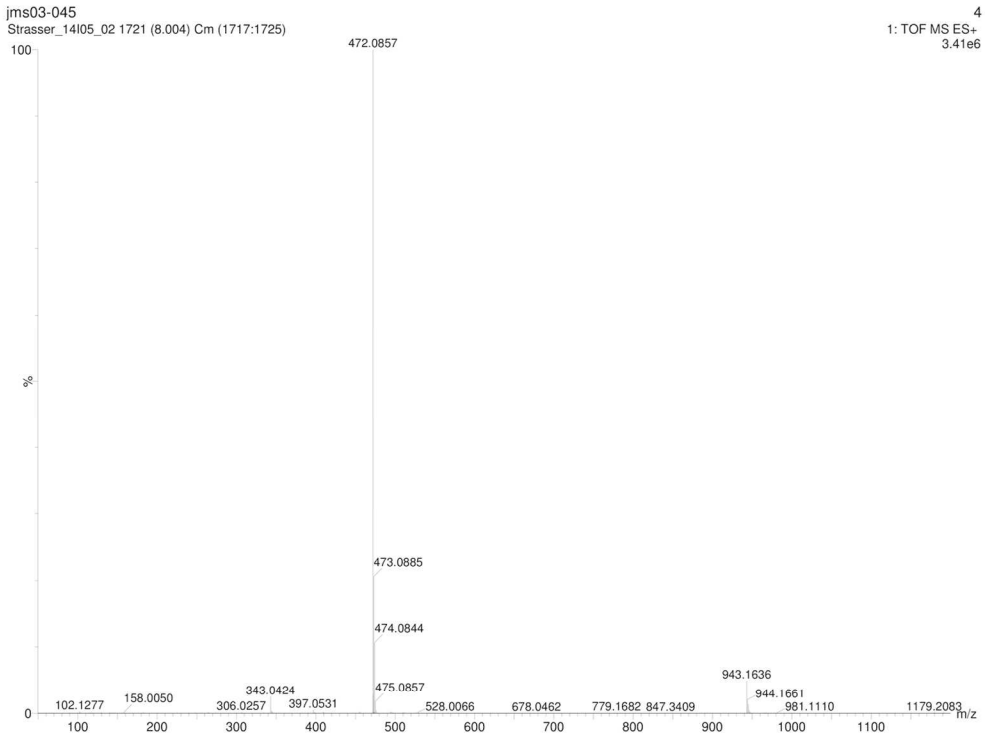

LC-HRMS, adduct **2a'** (via **2a** + GSH in HTS buffer)

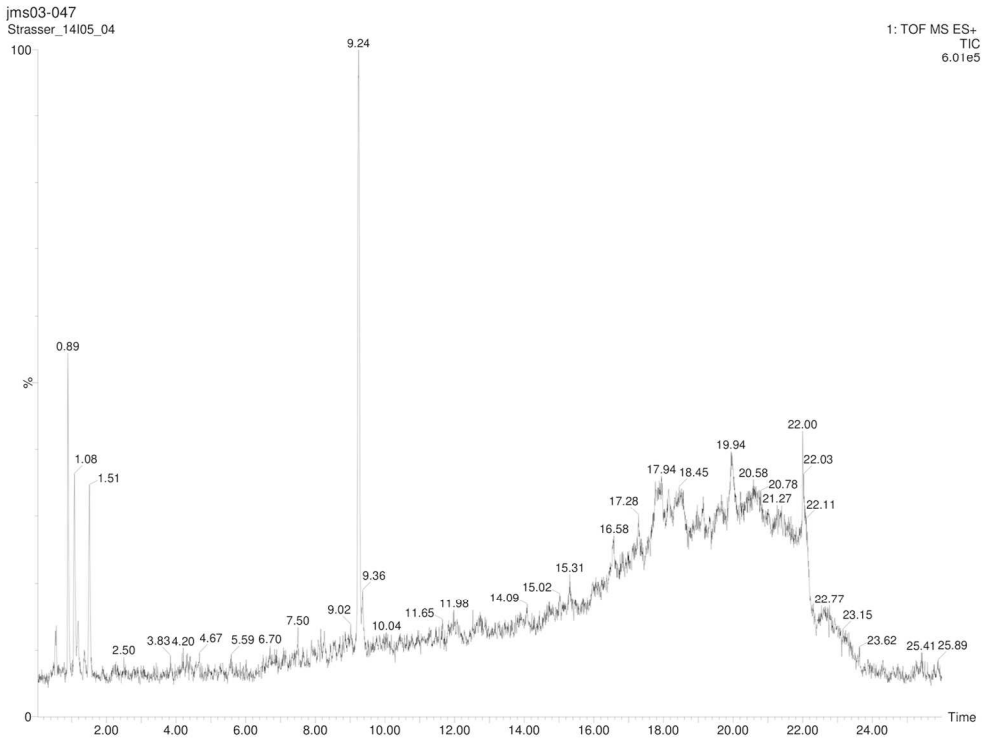

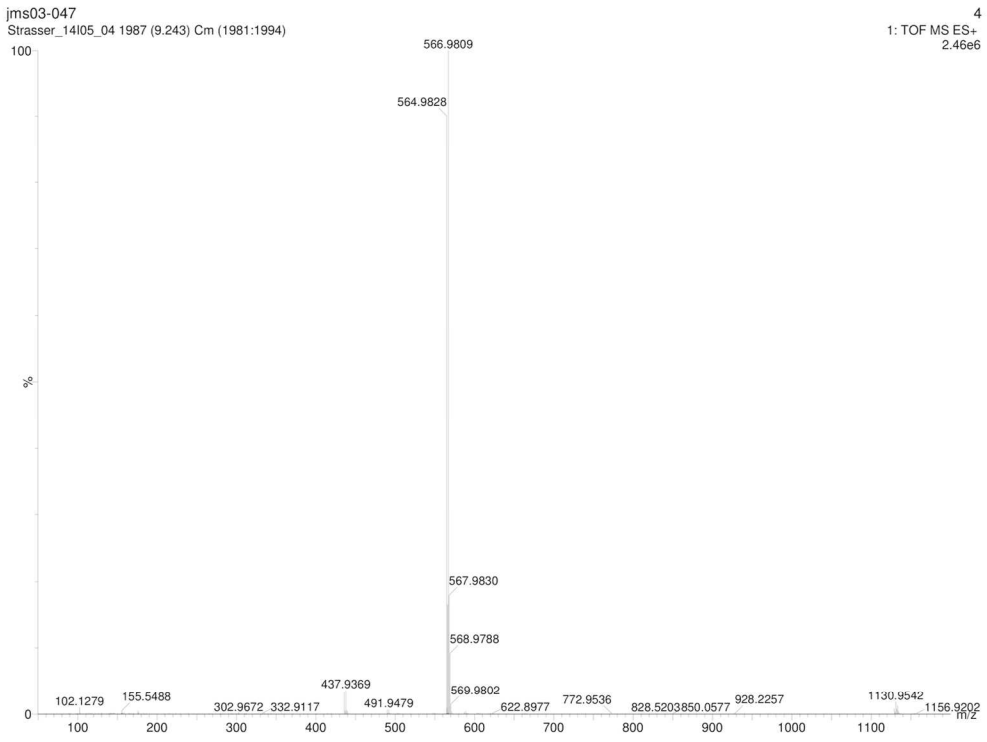

LC-HRMS, adduct **3a''** (via **3a** + GSH in HTS buffer)

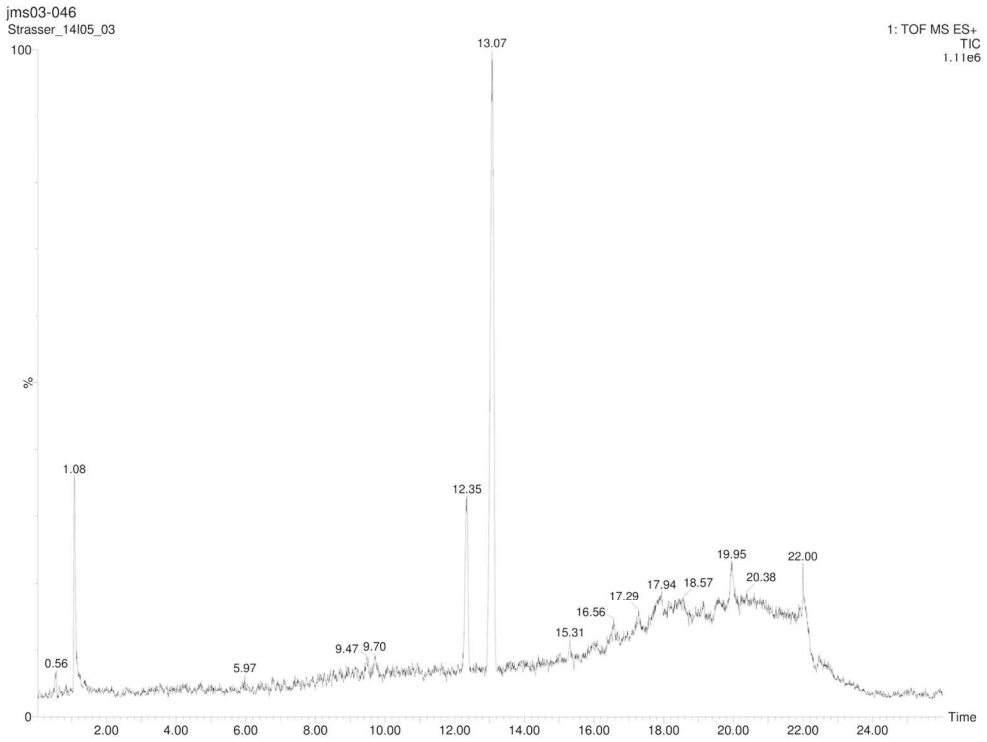

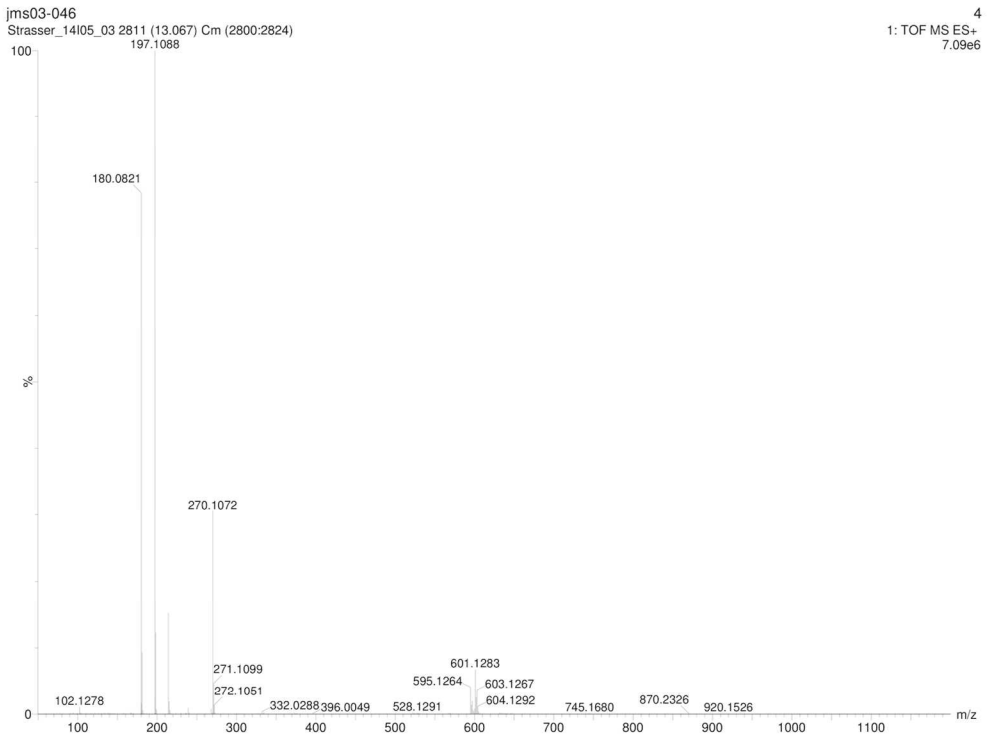

LC-HRMS, adduct **4a'** (via **4a** + GSH in HTS buffer)

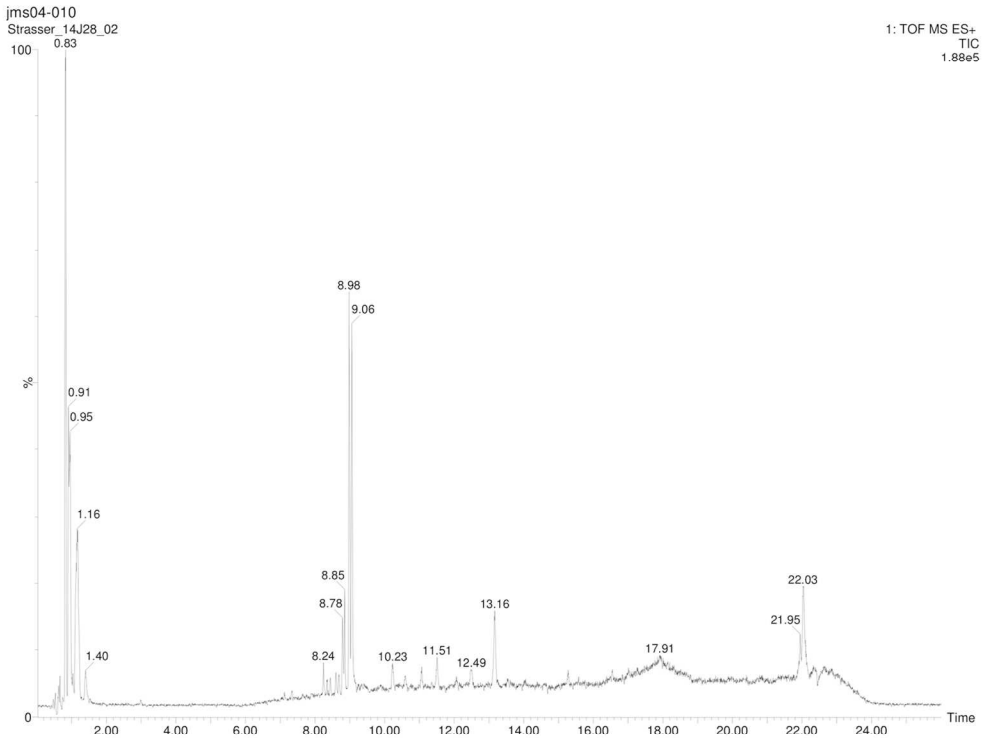

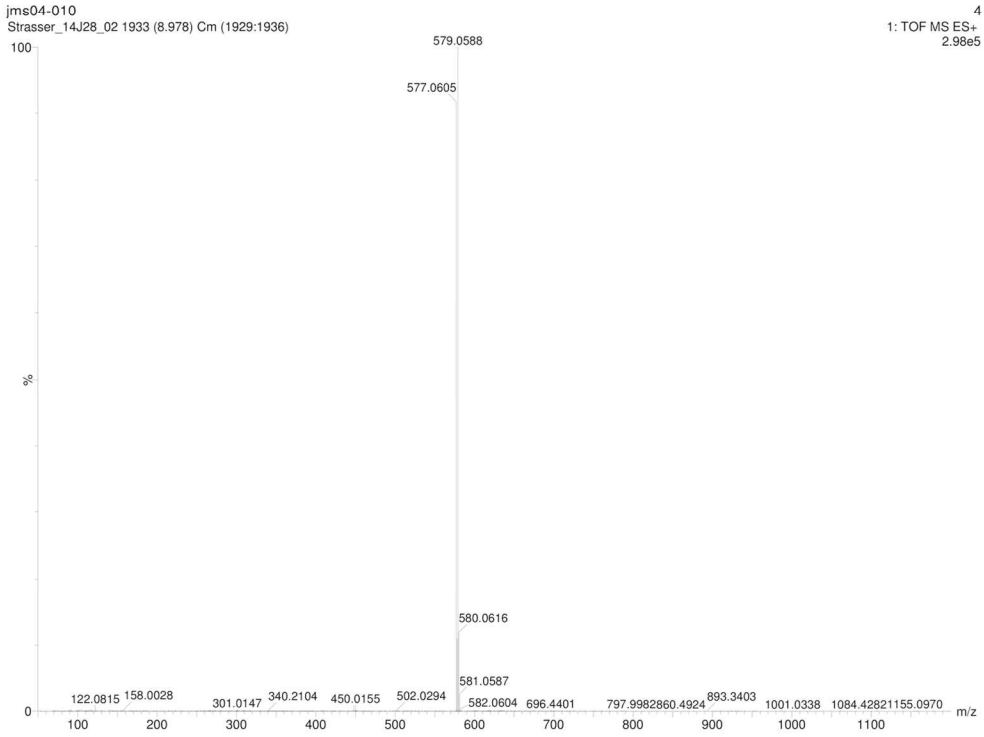

LC-HRMS, adduct **6''** (via **6a** + GSH in HTS buffer)

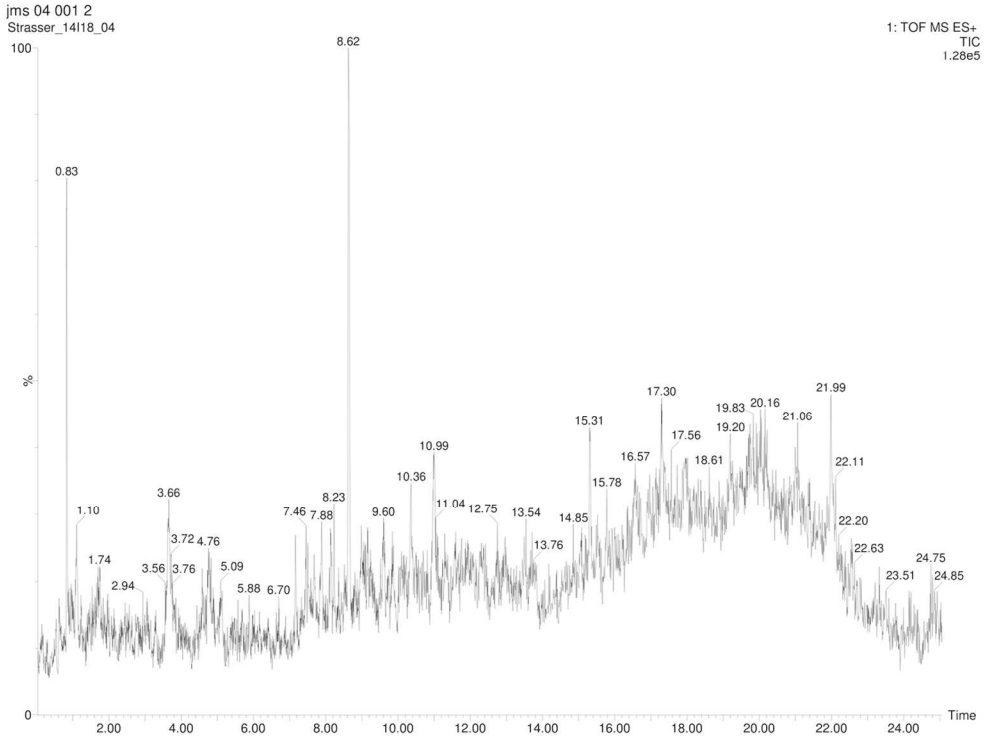

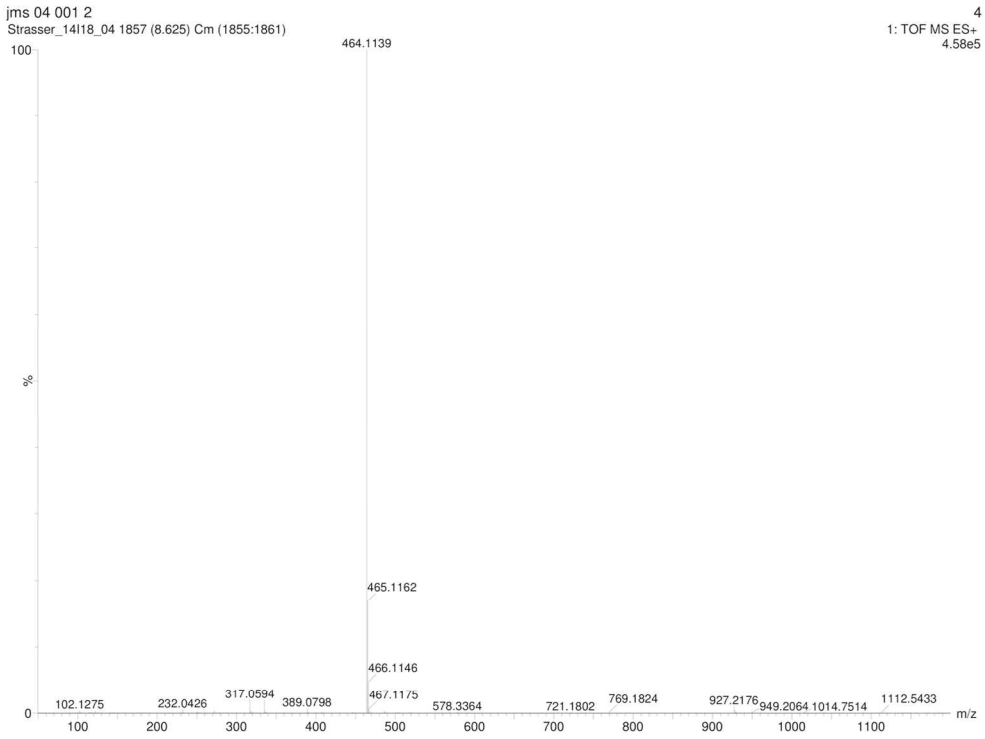

LC-HRMS, adduct **6''** (via **6b** + GSH in HTS buffer)

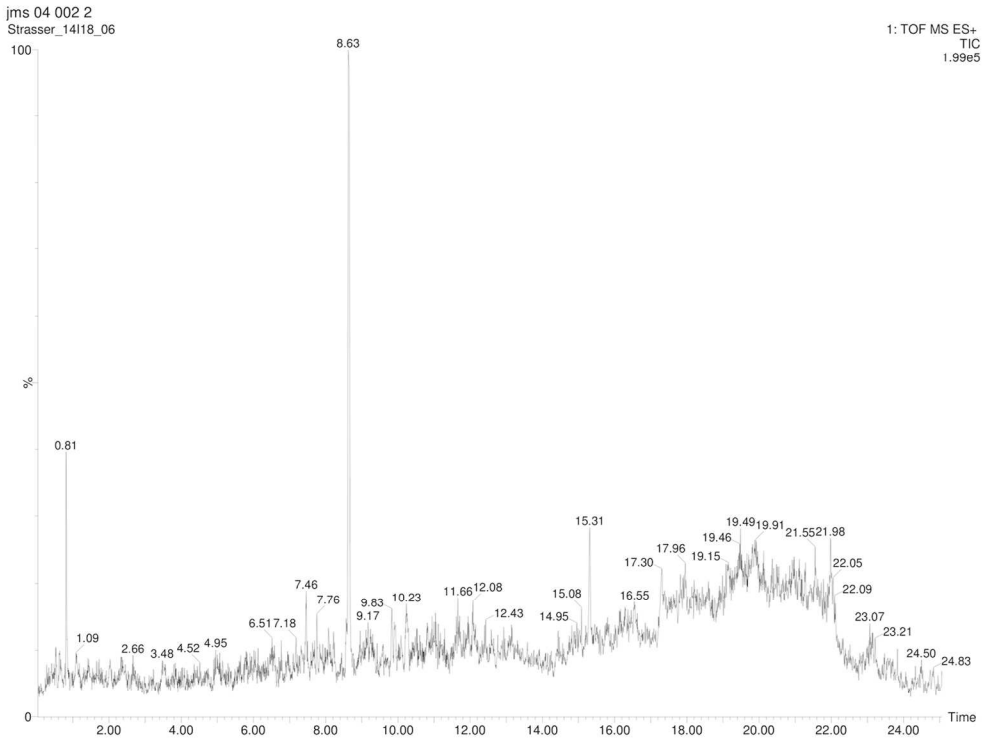

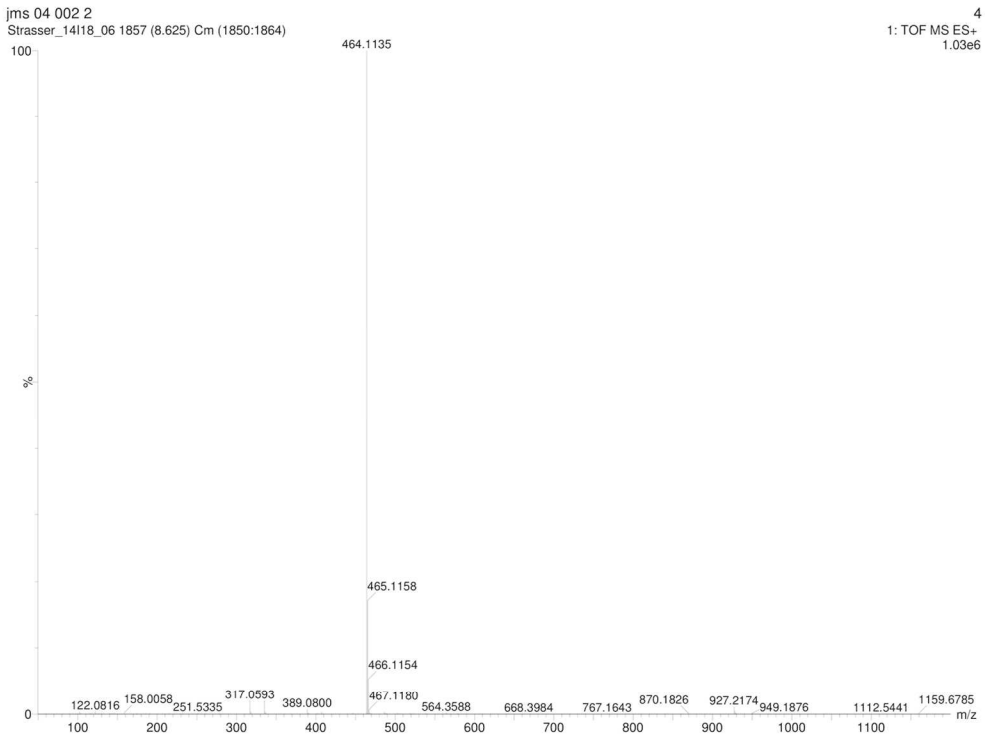

Examples of interference compounds reported in the scientific literature

Based on straightforward SciFinder searches, there are many examples of the problematic chemotypes described in this study (**1**, **2**, **3**, **4**, **6** and **7**) found in the scientific literature. Specifically, this includes benzothiophene 1,1-dioxides[7-9], *p*-hydroxyarylsulfonamides[2-5, 10-24], 1,2,4-thiadiazoles[25-44], 3-arylsulfonyl-succinimides[45, 46] and benzothiadiazoles/benzofurazans[47-59]. Some of these manuscripts only report compounds containing these chemotypes as being active in an HTS setting and make no further claims. Others, unfortunately, make rather dubious claims about the biological utility and specificity for these frequent-hitting interference compounds.

SUPPLEMENTAL REFERENCES

1. Zhang, J.; Xin, L.; Shan, B.; Chen, W.; Xie, M.; Yuen, D.; Zhang, W.; Zhang, Z.; Lajoie, G.; Ma, B. PEAKS DB: *de novo* sequencing assisted database search for sensitive and accurate peptide identification. *Mol. Cell. Proteomics* **2012,** 11, M111.010587.
2. Ge, Y.; Kazi, A.; Marsilio, F.; Luo, Y.; Jain, S.; Brooks, W.; Daniel, K. G.; Guida, W. C.; Sebti, S. M.; Lawrence, H. R. Discovery and synthesis of hydronaphthoquinones as novel proteasome inhibitors. *J. Med. Chem.* **2012,** 55, 1978−1998.
3. Xu, X.; Kasembeli, M. M.; Jiang, X.; Tweardy, B. J.; Tweardy, D. J. Chemical probes that competitively and selectively inhibit Stat3 activation. *PLoS One* **2009,** 4, e4783.
4. Abulwerdi, F.; Liao, C.; Liu, M.; Azmi, A. S.; Aboukameel, A.; Mady, A. S. A.; Gulappa, T.; Cierpicki, T.; Owens, S.; Zhang, T.; Sun, D.; Stuckey, J. A.; Mohammad, R. M.; Nikolovska-Coleska, Z. A novel small-molecule inhibitor of Mcl-1 blocks pancreatic cancer growth *in vitro* and *in vivo*. *Mol. Cancer Ther.* **2014,** 13, 565−575.
5. Qin, J.; Xie, P.; Ventocilla, C.; Zhou, G.; Vultur, A.; Chen, Q.; Liu, Q.; Herlyn, M.; Winkler, J.; Marmorstein, R. Identification of a novel family of $BRAF^{V600E}$ inhibitors. *J. Med. Chem.* **2012,** 55, 5220−5230.
6. Dalluge, J. J.; Connell, L. B. On the potential of mass spectrometry-based metabolite profiling approaches to the study of biochemical adaptation in psychrophilic yeast. *Extremophiles* **2013,** 17, 953−961.
7. Zhu, P.; Peng, H.; Ni, N.; Wang, B.; Li, M. Novel AI-2 quorum sensing inhibitors in *Vibrio harveyi* identified through structure-based virtual screening. *Bioorg. Med. Chem. Lett.* **2012,** 22, 6413−6417.
8. Ananthan, S.; Faaleolea, E. R.; Goldman, R. C.; Hobrath, J. V.; Kwonga, C. D.; Laughonc, B. E.; Maddrya, J. A.; Mehtaa, A.; Rasmussena, L.; Reynoldsa, R. C.; Secrist, J. A.; Shindoa, N.; Showeb, D. N.; Sosaa, M. I.; Sulinga, W. J.; Whitea, E. L. High-throughput screening for inhibitors of *Mycobacterium tuberculosis* H37Rv. *Tuberculosis* **2009,** 89, 334−353.
9. Iley, J.; Moreira, R.; Martins, L.; Guedes, R. C.; Soares, C. M. The Bsmoc group as a novel scaffold for the design of irreversible inhibitors of cysteine proteases. *Bioorg. Med. Chem. Lett.* **2006,** 16, 2738−2741.
10. Kilgore, J. A.; Du, X.; Melito, L.; Wei, S.; Wang, C.; Chin, H. G.; Posner, B.; Pradhan, S.; Ready, J. M.; Williams, N. S. Identification of DNMT1 selective antagonists using a novel scintillation proximity assay. *J. Biol. Chem.* **2013,** 288, 19673−19684.
11. Mori, M.; Tintori, C.; Christopher, R. S. A.; Marco Radi, S. S.; Musumeci, F.; Brullo, C.; Sanità, P.; Monache, S. D.; Angelucci, A.; Kissova, M.; Crespan, E.; Maga, G.; Botta, M. A combination strategy to inhibit Pim-1: synergism between noncompetitive and ATP-competitive inhibitors. *ChemMedChem* **2013,** 8, 484−496.
12. Zhang, L.; Wang, X.; Feng, J.; Jia, Y.; Xu, F.; Xu, W. Discovery of novel vascular endothelial growth factor receptor 2 inhibitors: a virtual screening approach. *Chem. Biol. Drug Des.* **2012,** 80, 893−901.
13. Jain, S. V.; Ghate, M.; Bhadoriya, K. S.; Bari, S. B.; Sugandhi, G.; Mandwal, P. 3D-QSAR pharmacophore modeling and in silico screening of phospholipase $A_{2\alpha}$ inhibitors. *Med. Chem. Res.* **2013,** 22, 3096−3108.
14. Preuss, J.; Hedrick, M.; Sergienko, E.; Pinkerton, A.; Mangravita-Novo, A.; Smith, L.; Marx, C.; Fischer, E.; Jortzik, E.; Rahlfs, S.; Becker, K.; Bode, L. High-throughput screening for small-molecule inhibitors of *Plasmodium falciparum* glucose-6-phosphate dehydrogenase 6-phosphogluconolactonase. *J. Biomol. Screening* **2012,** 17, 738−751.
15. Nagarajan, S.; Skoufias, D. A.; Kozielski, F.; Pae, A. N. Receptor-ligand interaction-based virtual screening for novel Eg5/kinesin spindle protein inhibitors. *J. Med. Chem.* **2012,** 55, 2561−2573.

16. Chou, T.-F.; Brown, S. J.; Minond, D.; Nordin, B. E.; Li, K.; Jones, A. C.; Chase, P.; Porubsky, P. R.; Stoltz, B. M.; Schoenen, F. J.; Patricelli, M. P.; Hodder, P.; Rosen, H.; Deshaies, R. J. Reversible inhibitor of p97, DBeQ, impairs both ubiquitin-dependent and autophagic protein clearance pathways. *Proc. Natl. Acad. Sci. U. S. A.* **2011,** 108, 4834−4839.
17. Alexiou, P.; Demopoulos, V. J. A diverse series of substituted benzenesulfonamides as aldose reductase inhibitors with antioxidant activity: design, synthesis, and *in vitro* activity. *J. Med. Chem.* **2010,** 53, 7756−7766.
18. Mallya, M.; Phillips, R. L.; Saldanha, S. A.; Gooptu, B.; Brown, S. C. L.; Termine, D. J.; Shirvani, A. M.; Wu, Y.; Sifers, R. N.; Abagyan, R.; Lomas, D. A. Small molecules block the polymerization of Z α_1-antitrypsin and increase the clearance of intracellular aggregates. *J. Med. Chem.* **2007,** 50, 5357−5363.
19. Barril, X.; Brough, P.; Drysdale, M.; Hubbard, R. E.; Massey, A.; Surgenor, A.; Wright, L. Structure-based discovery of a new class of Hsp90 inhibitors. *Bioorg. Med. Chem. Lett.* **2005,** 15, 5187−5191.
20. Xu, F.; Xu, H.; Wang, X.; Zhang, L.; Wen, Q.; Zhang, Y. Discovery of *N*-(3-((7*H*-purin-6-yl)thio)-4-hydroxynaphthalen-1-yl)-sulfonamide derivatives as novel protein kinase and angiogenesis inhibitors for the treatment of cancer: Synthesis and biological evaluation. Part III. *Bioorg. Med. Chem.* **2014,** 22, 1487−1495.
21. Larsen, M. J.; Larsen, S. D.; Fribley, A.; Grembecka, J.; Homan, K.; Mapp, A.; Haak, A.; Nikolovska-Coleska, Z.; Stuckey, J. A.; Sun, D.; Sherman, D. H. The role of HTS in drug discovery at the University of Michigan. *Comb. Chem. High Throughput Screening* **2014,** 17, 210−230.
22. Zhuang, C.; Narayanapillai, S.; Zhang, W.; Sham, Y. Y.; Xing, C. Rapid identification of Keap1-Nrf2 small-molecule inhibitors through structure-based virtual screening and hit-based substructure search. *J. Med. Chem.* **2014,** 57, 1121−1126.
23. Reed, D.; Shen, Y.; Shelat, A. A.; Arnold, L. A.; Ferreira, A. M.; Zhu, F.; Mills, N.; Smithson, D. C.; Regni, C. A.; Bashford, D.; Cicero, S. A.; Schulman, B. A.; Jochemsen, A. G.; Guy, R. K.; Dyer, M. A. Identification and characterization of the first small molecule inhibitor of MDMX. *J. Biol. Chem.* **2010,** 287, 10786−10796.
24. Vuorinen, A.; Engeli, R.; Meyer, A.; Bachmann, F.; Griesser, U. J.; Schuster, D.; Odermatt, A. Ligand-based pharmacophore modeling and virtual screening for the discovery of novel 17 β-hydroxysteroid dehydrogenase 2 inhibitors. *J. Med. Chem.* **2014,** 57, 5995−6007.
25. Morales-García, J. A.; Susín, C.; Alonso-Gil, S.; Pérez, D. I.; Palomo, V.; Pérez, C.; Conde, S.; Santos, A.; Gil, C.; Martinez, A.; Pérez-Castillo, A. Glycogen synthase kinase-3 inhibitors as potent therapeutic agents for the treatment of Parkinson disease. *ACS Chem. Neurosci.* **2013,** 4, 350−360.
26. Susín, C.; Morales-Garcia, J. A.; Aguilar-Morante, D.; Palomo, V.; Sanz-Sancristobal, M.; Alonso-Gil, S.; Gil, C.; Santos, A.; Martinez, A.; Perez-Castillo, A. The new iminothiadiazole derivative VP1.14 ameliorates hippocampal damage after an excitotoxic injury. *J. Neurochem.* **2012,** 122, 1193−1202.
27. Redondo, M.; Palomo, V.; Brea, J.; Pérez, D. I.; Martín-Álvarez, R.; Pérez, C.; Paúl-Fernández, N.; Conde, S.; Cadavid, M. I.; Loza, M. I.; Mengod, G.; Martinez, A.; Gil, C.; Campillo, N. E. Identification *in silico* and experimental validation of novel phosphodiesterase 7 inhibitors with efficacy in experimental autoimmune encephalomyelitis mice. *ACS Chem. Neurosci.* **2012,** 3, 793−803.
28. Palomo, V.; Pérez, D. I.; Pérez, C.; Morales-Garcia, J. A.; Soteras, I.; Alonso-Gil, S.; Encinas, A.; Castro, A.; Campillo, N. E.; Perez-Castillo, A.; Gil, C.; Martinez, A. 5-imino-1,2,4-thiadiazoles: first small molecules as substrate competitive inhibitors of glycogen synthase kinase 3. *J. Med. Chem.* **2012,** 55, 1645−1661.

29. Pérez, D. I.; Pistolozzi, M.; Palomo, V.; Redondo, M.; Fortugno, C.; Gil, C.; Felix, G.; Martinez, A.; Bertucci, C. 5-Imino-1,2-4-thiadiazoles and quinazolines derivatives as glycogen synthase kinase 3β (GSK-3β) and phosphodiesterase 7 (PDE7) inhibitors: determination of blood-brain barrier penetration and binding to human serum albumin. *Eur. J. Pharm. Sci.* **2012,** 45, 677−684.
30. Asami, Y.; Oishi, J.; Kitazaki, H.; Kamimoto, J.; Kang, J.-H.; Niidome, T.; Mori, T.; Katayama, Y. A simple set-and-mix assay for screening of protein kinase inhibitors in cell lysates. *Anal. Biochem.* **2011,** 418, 44−49.
31. Eisinger, M.; Li, W.-H.; Anthonavage, M.; Pappas, A.; Zhang, L.; Rossetti, D.; Huang, Q.; Seiberg, M. A melanocortin receptor 1 and 5 antagonist inhibits sebaceous gland differentiation and the production of sebum-specific lipids. *J. Dermatol. Sci.* **2011,** 63, 23−32.
32. Xia, M.; Guo, V.; Huang, R.; Shahane, S. A.; Austin, C. P.; Nirenberg, M.; Sharma, S. K. Inhibition of morphine-induced cAMP overshoot: a cell-based assay model in a high-throughput format. *Cell. Mol. Neurobiol.* **2011,** 31, 901−907.
33. Duckworth, B. P.; Aldrich, C. C. Development of a high-throughput fluorescence polarization assay for the discovery of phosphopantetheinyl transferase inhibitors. *Anal. Biochem.* **2010,** 403, 13−19.
34. Paterniti, I.; Mazzon, E.; Gil, C.; Impellizzeri, D.; Palomo, V.; Redondo, M.; Pérez, D. I.; Esposito, E.; Martinez, A.; Cuzzocrea, S. PDE 7 inhibitors: new potential drugs for the therapy of spinal cord injury. *PLoS One* **2011,** 6, e15937.
35. Shukla, S. J.; Nguyen, D.-T.; MacArthur, R.; Simeonov, A.; Frazee, W. J.; Hallis, T. M.; Marks, B. D.; Singh, U.; Eliason, H. C.; Printen, J.; Austin, C. P.; Inglese, J.; Auld, D. S. Identification of pregnane X receptor ligands using time-resolved fluorescence resonance energy transfer and quantitative high-throughput screening. *Assay Drug Dev. Technol.* **2009,** 7, 143−169.
36. Thompson, P. A.; Wang, S.; Howett, L. J.; Wang, M.-M.; Patel, R.; Averill, A.; Showalter, R. E.; Li, B.; Appleman, J. R. Identification of ligand binding by protein stabilization: comparison of ATLAS with biophysical and enzymatic methods. *Assay Drug Dev. Technol.* **2008,** 6, 69−81.
37. Gao, Z.-G.; Gross, A. S.; Jacobson, K. A. Effects of the allosteric modulator SCH-202676 on adenosine and P2Y receptors. *Life Sci.* **2004,** 74, 3173−3180.
38. Lanzafame, A.; Christopoulos, A. Investigation of the interaction of a putative allosteric modulator, *N*-(2,3-diphenyl-1,2,4-thiadiazole-5-(2*H*)-ylidene) methanamine hydrobromide (SCH-202676), with M_1 muscarinic acetylcholine receptors. *J. Pharmacol. Exp. Ther.* **2003,** 308, 830−837.
39. Nieuwendijk, A. M. C. H. v. d.; Pietra, D.; Heitman, L.; Göblyös, A.; IJzerman, A. P. Synthesis and biological evaluation of 2,3,5-substituted [1,2,4]thiadiazoles as allosteric modulators of adenosine receptors. *J. Med. Chem.* **2004,** 47, 663−672.
40. Hardy, R. W.; Marcotrigiano, J.; Blight, K. J.; Majors, J. E.; Rice, C. M. Hepatitis C virus RNA synthesis in a cell-free system isolated from replicon-containing hepatoma cells. *J. Virol.* **2003,** 77, 2029−2037.
41. Pan, K.; Scott, M. K.; Lee, D.; Fitzpatrick, L. J. 2,3-Diaryl-5-anilino [1,2,4] thiadiazoles as melanocortin MC4 receptor agonists and their effects on feeding behavior in rats. *Bioorg. Med. Chem.* **2003,** 11, 185−192.
42. Fawzi, A. B.; Macdonald, D.; Benbow, L. L.; Smith-Torhan, A.; Zhang, H.; Weig, B. C.; Ho, G.; Tulshian, D.; Linder, M. E.; Graziano, M. P. SCH-202676: An allosteric modulator of both agonist and antagonist binding to G protein-coupled receptors. *Mol. Pharmacol.* **2001,** 59, 30−37.
43. Castro, A.; Castaño, T.; Encinas, A.; Porcal, W. Advances in the synthesis and recent therapeutic applications of 1,2,4-thiadiazole heterocycles. *Bioorg. Med. Chem.* **2006,** 14, 1644−1652.

44. Morales-Garcia, J. A.; Palomo, V.; Redondo, M.; Alonso-Gil, S.; Gil, C.; Martinez, A.; Perez-Castillo, A. Crosstalk between phosphodiesterase 7 and glycogen synthase kinase-3: two relevant therapeutic targets for neurological disorders. *ACS Chem. Neurosci.* **2014,** 5, 194−204.
45. Sonawane, N. D.; Verkman, A. S. Thiazolidinone CFTR inhibitors with improved water solubility identified by structure-activity analysis. *Bioorg. Med. Chem.* **2008,** 16, 8187−8195.
46. Xu, D.; Jiang, B.; Ketela, T.; Lemieux, S.; Veillette, K.; Martel, N.; Davison, J.; Sillaots, S.; Trosok, S.; Bachewich, C.; Bussey, H.; Youngman, P.; Roemer, T. Genome-wide fitness test and mechanism-of-action studies of inhibitory compounds in *Candida albicans*. *PLoS Pathog.* **2007,** 3, e92.
47. Baell, J. B.; Holloway, G. A. New substructure filters for removal of pan assay interference compounds (PAINS) from screening libraries and for their exclusion in bioassays. *J. Med. Chem.* **2010,** 53, 2719−2740.
48. Metz, J. T.; Huth, J. R.; Hajduk, P. J. Enhancement of chemical rules for predicting compound reactivity towards protein thiol groups. *J. Comput. -Aided Mol. Des.* **2007,** 21, 139−144.
49. Huth, J. R.; Mendoza, R.; Olejniczak, E. T.; Johnson, R. W.; Cothron, D. A.; Liu, Y.; Lerner, C. G.; Chen, J.; Hajduk, P. J. ALARM NMR: a rapid and robust experimental method to detect reactive false positives in biochemical screens. *J. Am. Chem. Soc.* **2005,** 127, 217−224.
50. Kessler, U.; Castagnolo, D.; Pagano, M.; Deodato, D.; Bernardini, M.; Pilger, B.; Ranadheera, C.; Botta, M. Discovery and synthesis of novel benzofurazan derivatives as inhibitors of influenza A virus. *Bioorg. Med. Chem. Lett.* **2013,** 23, 5575−5577.
51. Xie, F.; Li, B. X.; Broussard, C.; Xiao, X. Identification, synthesis and evaluation of substituted benzofurazans as inhibitors of CREB-mediated gene transcription. *Bioorg. Med. Chem. Lett.* **2013,** 23, 5371−5375.
52. Galano, J. J.; Alías, M.; Pérez, R.; Velazquez-Campoy, A.; Hoffman, P. S.; Sancho, J. Improved flavodoxin inhibitors with potential therapeutic effects against *Helicobacter pylori* infection. *J. Med. Chem.* **2013,** 56, 6248−6258.
53. Tholander, F.; Sjöberg, B.-M. Discovery of antimicrobial ribonucleotide reductase inhibitors by screening in microwell format. *Proc. Natl. Acad. Sci. U. S. A.* **2012,** 109, 9798−9803.
54. Durk, R. C.; Singh, K.; Cornelison, C. A.; Rai, D. K.; Matzek, K. B.; Leslie, M. D.; Schafer, E.; Marchand, B.; Adedeji, A.; Michailidis, E.; Dorst, C. A.; Moran, J.; Pautler, C.; Rodriguez, L. L.; McIntosh, M. A.; Rieder, E.; Sarafianos, S. G. Inhibitors of foot and mouth disease virus targeting a novel pocket of the RNA-dependent RNA polymerase. *PLoS One* **2010,** 5, e15049.
55. Cosconati, S.; Hong, J. A.; Novellino, E.; Carroll, K. S.; Goodsell, D. S.; Olson, A. J. Structure-based virtual screening and biological evaluation of *Mycobacterium tuberculosis* a 5'-phosphosulfate reductase inhibitors. *J. Med. Chem.* **2008,** 51, 6627−6630.
56. Turella, P.; Filomeni, G.; Dupuis, M. L.; Ciriolo, M. R.; Molinari, A.; Maria, F. D.; Tombesi, M.; Cianfriglia, M.; Federici, G.; Ricci, G.; Caccuri, A. M. A strong glutathione *S*-transferase inhibitor overcomes the P-glycoprotein-mediated resistance in tumor cells. 6-(7-Nitro-2,1,3-benzoxadiazol-4-ylthio)hexanol (NBDHEX) triggers a caspase-dependent apoptosis in MDR1-expressing leukemia cells. *J. Biol. Chem.* **2006,** 281, 23725−23732.
57. Whitehouse, M. W.; Ghosh, P. B. 4-nitrobenzofurazans and 4-nitrobenzofuroxans: a new class of thiol-neutralising agents and potent inhibitors of nucleic acid synthesis in leucocytes. *Biochem. Pharmacol.* **1968,** 17, 158−161.
58. Ghosh, P. B.; Whitehouse, M. W. Potential antileukemic and immunosuppressive drugs. Preparation and *in vitro* pharmacological activity of some 2,1,3-benzoxadiazoles (benzofurazans) and their *N*-oxides (benzofuroxans). *J. Med. Chem.* **1968,** 11, 305−311.
59. Berkson, R. G.; Hollick, J. J.; Westwood, N. J.; Woods, J. A.; Lane, D. P.; Lain, S. Pilot screening programme for small molecule activators of p53. *Int. J. Cancer* **2005,** 115, 701−710.